이학박사 학위논문

# An integrated system for simulation and image-guidance for orthognathic surgery

악교정 수술에서 시뮬레이션 및 영상 가이드를 제공하는 통합 시스템

2013 년 8 월

서울대학교 대학원

협동과정 방사선응용생명과학 전공

김 대 승

# 악교정 수술에서 시뮬레이션 및 영상 가이드를 제공하는 통합 시스템

지도교수 이 원 진

이 논문을 이학박사 학위논문으로 제출함
2013년 8월

서울대학교 대학원
협동과정 방사선응용생명과학 전공
김 대 승

김대승의 이학박사 학위논문을 인준함
2013년 7월

위 원 장 황 순 정 (인)

부위원장 이 원 진 (인)

위 원 이 삼 선 (인)

위 원 이 재 성 (인)

위 원 배 유 석 (인)

# An integrated system for simulation and image-guidance for orthognathic surgery

by

**Dae Seung Kim**

**A thesis submitted to the Interdisciplinary Graduate Program in partial fulfillment of the requirements for the Degree of Doctor of Philosophy in Radiation Applied Life Science at Seoul National University**

**Seoul, Korea**

**July 2013**

**Approved by Thesis Committee:**

| | | |
|---|---|---|
| **Chairman** | Soon Jung Hwang | _____ |
| **Vice chairman** | Won Jin Yi | _____ |
| **Member** | Sam Sun Lee | _____ |
| **Member** | Jae Sung Lee | _____ |
| **Member** | You Suk Bae | _____ |

# ABSTRACT

## An integrated system for simulation and image-guidance for orthognathic surgery

**Dae seung Kim**

**Interdisciplinary Program**

**in Radiation Applied life science**

**The Graduate School**

**Seoul National University**

Accurate orthognathic surgery planning and planning transfer in the operation theatre are important factors for a successful surgery outcome with appropriate esthetical and functional improvements. However, conventional surgery has inherent limitations because the surgery planning is performed based on 2-dimensional cephalograms and the surgery operation depends on the experience and skill of surgeons. Moreover, 3-dimensional natural head position (NHP) information was not contained in not only the cephalogram

but also CT data. To overcome these limitations, a new integrated system covering from virtual surgery planning to surgery guide system for orthognathic surgery has been developed. A new method for 3-dimensional simulation of NHP was also developed using POSIT algorithm. An accuracy evaluation was performed for the NHP simulation and the surgery guide system.

In the virtual surgery planning system, realistic virtual osteotomy was performed on a 3-dimensional surface model reconstructed from the CT data using a haptic device. After designation of the landmarks on the surface model for a bone relocation procedure, bone segment was relocated by a combination of rotational and translational movements for each axis. The simulation of bone segment relocation was done according to the conventional surgery planning method. Movements of the designated landmarks were calculated for each relocation step and the final positions of the landmarks were compared with the conventional surgery plan to verify the simulation result. Relocated final position of the bone segment was recorded for the surgery guide system.

For the NHP simulation, a photograph of subject was taken after attaching ceramic sphere markers on the subject's maxillofacial area. CT data of the subject was also acquired while the ceramic markers were attached on the same positions. The POSIT algorithm was performed to acquire the

relationship between the photograph coordinate system and the CT coordinate system. The 2-dimensional and 3-dimensional marker positions were acquired from the photograph and the CT data, respectively, and these positions were used for the POSIT algorithm calculation. The transformation matrix between the two coordinate systems was acquired as a result of the transformation calculation. Acquired transformation was applied to the CT data of the subject and the CT data was reoriented to the NHP.

A Phantom was designed for an accuracy evaluation of the NHP simulation. Discrepancy between the simulated orientation and a virtual NHP of the phantom was determined as an accuracy of the simulation. The result of the accuracy evaluation of the NHP simulation showed clinically acceptable errors (degree) with 0.05±0.19 in roll, -0.56±0.37 in pitch and -0.01±0.29 in yaw. Intra-observer and inter-observer variation was evaluated for the NHP simulation and showed good agreement between measurements ($p$-value = 0.05).

The surgery guide system tracked the maxilla bone segment intra-operatively using a 3-dimensional optical tracking system. Specially designed registration body was fabricated to improve the efficiency of the surgery. The point-to-point registration method was implemented to acquire the relationship between the optical tracking system coordinate system and the CT coordinate system. With the help of newly developed registration body,

the registration procedure could be performed preoperatively. After the registration was completed, real-time maxilla bone segment position was tracked by the system. The result of the surgery planning which was previously acquired from the virtual surgery planning system was imported into the surgery guide system. During the tracking procedure, discrepancy between the planned position and the real-time intraoperative position of the maxilla bone segment was shown in 3-dimensional virtual environment. The discrepancy information of the points of interests on the bone segment was also quantitatively calculated.

An accuracy of the surgery guide system was evaluated and compared with the conventional surgery guide method. The mean error was 0.47 ± 0.22 mm for the developed method and 1.05 ± 0.49 mm for the conventional method. The error of the developed method was significantly lower than the conventional method for all direction of movements. The accuracy of the surgery guide system was also evaluated in more clinical condition using the result of the model surgery. The CT data of the patient's dental casts was acquired with the registration assembly. Registration between the CT coordinate system and the articulator coordinate system was performed, and the surface model of the dental cast was reoriented to the articulator coordinate system. The maxilla bone segment was relocated according to the model surgery result and tracked by the surgery guide system. Discrepancy of

the landmark positions between the virtual surgery planned position and the actual position according to the model surgery was calculated and used for the evaluation of the system accuracy. Total of 7 cases of experiment was done and 5 measurements were implemented on 8 landmarks for each case. Total average of the absolute error ranged from 0.06 to 0.87 mm and the RMS error was 0.54±0.21 mm. The evaluation results showed clinically acceptable accuracy.

In this study, integrated system for orthognathic surgery was developed. The system contained the virtual surgery planning system, the NHP simulation and the surgery guide system. The developed system helped the surgeons to predict the result of orthognathic surgery preoperatively and verify the exact intraoperative transfer of the surgery planning.

In conclusion, this system was compatible with the clinical environment and increased the efficiency and the accuracy of the orthognathic surgery from the surgery planning to the surgery operation. The developed system is expected to be adopted in routine clinical situation and could be useful for the overall improvements of facial deformities after surgery.

**Keywords:** Orthognathic surgery, Natural head position simulation, Virtual surgery simulation, Surgery guide system

**Student Number:** 2009-30596

# CONTENTS

# LIST OF TABLES

# LIST OF FIGURES

# INTRODUCTION

Orthognathic surgery is performed to improve facial esthetics and masticatory function of patients with facial deformities. Accurate orthognathic surgery planning and operation are important factors for successful surgery with the appropriate esthetical and functional improvements. However, surgery results still mostly depend on the experience and ability of the surgeons and surgery treatment and operation methods have not much improved over the decades. While the surgery is one on 3-dimensional complex structures, surgery planning is still performed based on 2-dimensional radiographs and model surgery is implemented using dental plaster casts and a mechanical articulator. During operations, surgeons transfer the surgery plan based on 2-dimensional paper surgery, and calipers and rulers are used to identify the relocated position of the bone segments, which can lead to inaccurate surgery results especially when the patients have severe and complex facial deformities. Recent developments in 3-dimensional medical imaging, computer graphics and tracking technology have increased the possibility of adopting a computer aided system for use in a clinical environment. Several computer aided surgery systems for maxillofacial area surgery have been developed to overcome the inaccuracy and inconvenience

of conventional surgical methods (1-8). Especially, an integrated system ranging from diagnosis and planning to surgery operation is needed to improve and ensure the accuracy of the final outcome.

Conventionally paper surgery and model surgery were used as a means of orthognathic surgery planning. Paper surgery was performed based on a 2-dimensional cephalometric radiograph and the result of the paper surgery was simulated using dental casts and an articulator in a model surgery procedure. A complex 3-dimensional bone relocation procedure was simplified to a combination of 2-dimensional movements in paper surgery. In model surgery, surgical outcome was realized 3-dimensionally, however, only information on the dental region change was provided and prediction of the whole skeletal change is unavailable (9-11). These limitations of conventional surgery planning may lead to an inaccurate surgery planning when facial asymmetry exists because complicated combinations of movements are involved for asymmetric cases (12).

Recently, computer-aided surgery planning for the maxillofacial area was introduced for a more accurate prediction of surgical outcome with the help of advances in virtual reality and computer graphic technology (13-22). In previous studies on virtual orthognathic surgery, however, exact simulation of realistic osteotomy including collision detection was unavailable and the virtual surgery was not performed based on the conventional paper surgery

procedure. This can lead to an inaccurate and unreliable surgery simulation and, therefore, discourage surgeons from adopting the virtual surgery system. By applying realistic osteotomy combined with collision detection, more accurate prediction of the bone interference can be acquired and osteotomy lines could be adjusted according to the prediction result. Realistic osteotomy and exact simulation of surgery according to the conventional surgery plan are necessary to increase the reliability and clinical routine adoption of a virtual surgery prediction system.

Recently, 3-dimensional CT imaging has been used for diagnosis and surgery planning for orthognathic surgery. However, orthognathic surgery based on CT data has a limitation because natural head position (NHP) is not reflected in the CT data. NHP is the relaxed head position when the eyes are focused on a distant horizon (23, 24) and considered as a logical reference for the evaluation of facial morphology (25-27). NHP has been reported to have reliable reproducibility in 2-dimension (24, 28, 29) and recently, 3-dimensional record of NHP was also found to be reproducible (30). There have been other reference lines or planes used for the analysis of facial morphology such as sella-nasion and Frankfort horizontal plane. However, those references were reported to be unreliable and have the possibility of misleading the analysis results and lower the reproducibility compared to NHP (23, 31, 32). Therefore, the accurate acquisition of NHP is important for

the diagnosis and treatment of maxillofacial deformities, especially for significant facial asymmetry cases (33). Simulation of NHP on the CT data is expected to improve the orthognathic surgery results. There have been several studies on the NHP of 2-dimensional cephalograms (34-38), but few studies have been performed for 3-dimensional data (39, 40). Previous studies on 3-dimensional NHP simulation used an expensive laser scanning device and extra tool mounted on the patient's mouth, discoursing clinical application (39, 40). Therefore, development of a simple and economic method with acceptable accuracy is needed.

The exact transfer of the surgery plan to the operative theatre is a crucial point for a surgery guide system. Techniques were developed to guarantee a more accurate transfer of surgery planning and surgical outcome including a simple template-based method (41). However, real-time tracking of the bone segment is more preferable than a pre-determined non-flexible method for surgeons to deal with complex 3-dimensional structures and operation environment. Recently, a 3-dimensional optical tracking system has been widely used for a surgery guide system because of its accuracy and reliability. A previously developed orthognathic surgery guide system verified the position of relocated bone segments by manually checking the position of anatomical landmark on the bone segment with a prove tool, which incurred the inconvenience and inaccuracy of the tracking procedure. In a more

developed orthognathic surgery guide system, movement of the maxilla was tracked and the discrepancy between the goal position and current position was calculated and displayed on the screen (14). Although, in that system the discrepancy information was represented as 6 degrees of freedom, it was not intuitive to surgeons to comprehend the situation because surgeons transfer the plan based on the position of landmarks. In this study, the maxilla bone segments were tracked by a 3-dimensional optical tracking system and a specially designed tool and method were developed to improve the efficiency of the surgery and the convenience of the method to the surgeons. The discrepancy between the goal and current position of the bone segment was calculated based on multiple landmark points to increase the surgeon's understanding about the situation.

Developed registration and tracking techniques were previously applied to temporomandibular joint movement tracking and simulation of mandibular movement (42 – 46). With the help of 3-dimensional tracking and simulation techniques, movement of the mandible was recorded and simulated, and the relationship between the 3-dimensional mandibular movement and facial morphology could be found. It was shown that the 3-dimensional mandibular movement was significantly correlated with the facial morphology and, up to 65% of the variation in facial morphology or combination of facial morphologies could explain the variation of the mandibular movement (45).

Moreover, the degree of changes in facial morphology according to the orthognathic surgery was associated with the changes in the mandibular movement (43).

In this study, an integrated system for surgery planning including NHP simulation and a surgery guide system was developed. This study focused on the development of the system which is compatible to clinical situations. Newly developed methods were introduced to improve the efficiency of the surgery and the convenience of the method to surgeons. The surgery planning system was compatible with the conventional surgery planning method and the NHP simulation method was simple to apply. The surgery guide system was developed to be applicable to a clinical environment and to ensure the exact transfer of the surgery planning.

# MATERIALS AND METHODS

## 1. Virtual surgery planning system

1) Virtual osteotomy

A virtual surgery planning system was developed to simulate the relocation procedure of bone segments quantitatively. A three-dimensional surface model of the skull was constructed from CT data using the threshold technique. Then, virtual osteotomy was performed on the surface model of the patient's skull. Virtual osteotomy was implemented with a 3-dimensional modeling program (Freeform modeling, Sensable group, Wilmington, USA) and 3-dimensional haptic device (PHANTOM Omni, Sensable group, Wilmington, USA). A reconstructed surface model was imported into the modeling program and converted to a volume model. Using the haptic device, users were able to freely manipulate the 3-dimensional model in the virtual environment with a tactile impression on the surface of the model. A cutting plane was positioned between the maxillary and mandibular teeth to separate the mandible from the skull. Two cutting planes were used to simulate Le-Fort I osteotomy. In addition to the simple cutting planes, cutting curves were

created to apply a more realistic Le-Fort I osteotomy because the part of the lateral pterygoid plate remained un-resected from the maxilla when only two cutting planes were used. By assigning points on the surface along the line between the maxilla and the lateral pterygoid plate, the maxilla was completely removed from the skull. Then, the resected part of the lateral pterygoid plate was merged into the skull model and the realistic Le-Fort I osteotomy simulation was completed. Sagittal split ramus osteotomy (SSRO) was simulated on the mandible with cutting curves through the assigned points on the surface to form a closed path of cutting. With the haptic device, surgeons could execute the virtual osteotomy and freely draw osteotomy curves on the surface with a tactile impression.

2) Bone segment relocation

From the virtual osteotomy, the skull model was divided into bone segment models and saved in STL (Stereolithography) model format. These bone segment models were loaded onto the virtual surgery planning system. Surface visualization and data manipulation in the virtual surgery planning system was implemented by the Visualization Toolkit (VTK, Kitware Inc., New York, USA). Landmarks for bone segment relocation were designated on the model according to the result of the paper surgery. After landmark designation was finished, translational and rotational movements were

performed quantitatively in 6 degrees of freedom according to the conventional surgery plan. A user entered the desired amount of movement through the GUI of the program.

Translational movement was implemented by moving bone segments by a given amount of distance for each direction. Especially for rotational movement, two landmarks were chosen: the rotation center and rotation target. The bone segment was rotated about the rotation center and the degree of rotation was given by the displacement of the rotation target in *mm* unit along each axis not by angular degree. Designating the amount of translational movement instead of the angular degree in rotational situation is the same way the conventional surgery plan treated the rotational movement. Rotation angle was calculated mathematically from the designated amount of translational movement considering the geometrical relationship between the rotation center and rotation target (Figure 1). In Figure 1, roll movement was described; $T(T_x, T_y, T_z)$: target center; $R(R_x, R_y, R_z)$: rotation center; *D*: required displacement; G: goal position; $\theta$: required rotation angle; *l*: the radius of rotation. Simple rotation of the target point, *T* about the rotation center, *R* moved *T* to *t*, not goal position *G*. Therefore, the compensational movement of *C* needed to be added for an accurate simulation. Rotation angle and compensational movement were calculated according to the following

equations.

$$l = \sqrt{(T_x - R_x)^2 + (T_y - R_y)^2 + (T_z - R_z)^2} \quad (1)$$

$$\theta_1 = sin^{-1}\left(\frac{D_t}{l}\right), D_t = T_z \quad (2)$$

$$\theta_2 = sin^{-1}\left(\frac{D_t + D}{l}\right) \quad (3)$$

$$\theta = \theta_2 - \theta_1 \quad (4)$$

$$C = T_x - l \times \cos(\theta_2) \quad (5)$$

3) Virtual surgery procedure

The surgery planning procedure was simulated in the virtual surgery planning system. Translational and rotational (roll, pitch and yaw) movements were performed according to the aforementioned manner. The amounts of displacements for each landmark were shown during relocation procedure. At each step of the bone segment relocation procedure, the amount of displacement for each landmark from the initial position were calculated and compared with the conventional surgery plan to confirm the accurate simulation of the virtual surgery. The final position and quantitative movement of the landmarks were confirmed and the positions of the bone segments were recorded.

4) Collision detection

After the relocation procedure was completed, collision detection was performed using the OBB (Oriented Bounding Boxes) algorithm. The OBB algorithm built a hierarchical OBB tree and computed the intersection between the OBBs to efficiently identify the collision between the polygons. The lines of intersection between bone segments were drawn on the surfaces of the bone segments, and possible area of collision and degrees of collision between bone segments could be identified prior to the actual surgery. The transparency of the selected surface model could be adjusted to enable a more close observation of the interference area.

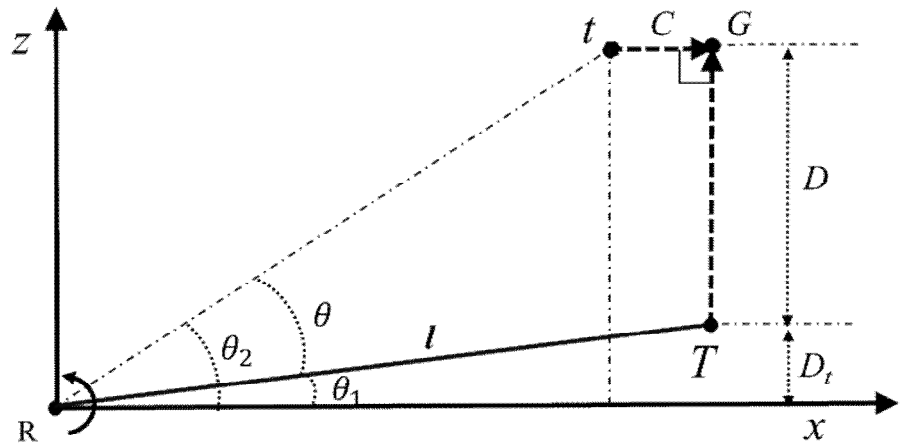


**Figure 1 V**irtual bone movement procedure for roll movement. Geometrical relationship between target center: *T*, Rotation center: *R*, Goal position: G, Compensational movement: *C*, Required rotation angle: $\theta$, Radius of rotation: *l,* Required displacement: *D*.

## 2. Natural head position simulation

1) POSIT algorithm

POSIT algorithm was used to record the NHP of a patient. Using the POSIT algorithm, a pose of a 3-dimensional object can be calculated from a 2-dimensional image. The POSIT algorithm is a combination of two algorithms, POS (Pose from Orthography and Scaling) and POS with ITeration (POSIT) (47). The POSIT algorithm calculates the pose of a 3-dimensional object quickly within a few iterations and does not require an initial pose. The POSIT algorithm is based on scaled orthographic projection (SOP) and the underlying basic theory is briefly illustrated in Figure 2. In Figure 2, $P_0$ is the reference point for object and $P_0, P_1, \ldots, P_i, \ldots, P_n$ are the feature points of the object with camera coordinates ($X_i$, $Y_i$, $Z_i$). O is the center of projection and f is the focal length. The scaled orthographic projection of $P_i$ is $S_i$, and the perspective projection of point $P_i$ and $S_i$ on the image plane is $p_i$ and $s_i$, respectively. In SOP, it is assumed that the depths of $P_i$ are not much different from each other and, all the feature points of the object and have the same depth of $Z_0$. In SOP, $P_i$ of the object is projected at a point $s_i$ on the image plane with the coordinates ($x'_i = f X_i / Z_0$, $y'_i = f Y_i / Z_0$), while, in perspective projection, $p_i$ is the projection of $P_i$ with the coordinates ($x_i = f X_i /$

$Z_i$, $y_i = f\ Y_i\ /\ Z_i$). When i and j are the first two row vectors of the rotation matrix, basic equations of the POSIT algorithm are shown as follows in equations (Eq. 6,7 and 8).

$$P_0P_i \cdot \frac{f}{Z_0}\mathrm{i} = x_i(1+\varepsilon_i) - x_0 \tag{6}$$

$$P_0P_i \cdot \frac{f}{Z_0}\mathrm{j} = y_i(1+\varepsilon_i) - y_0 \tag{7}$$

$$\varepsilon_i = \frac{1}{Z_0}P_0P_1 \cdot \mathrm{k} \tag{8}$$

with $\mathrm{k} = \mathrm{i} \times \mathrm{j}$

These equations were proven previously (47) and equations (6) and (7) can be written as

$$P_0P_i \cdot \mathrm{I} = x_i(1+\varepsilon_i) - x_0 \tag{9}$$

$$P_0P_i \cdot \mathrm{J} = y_i(1+\varepsilon_i) - y_0 \tag{10}$$

with $\mathrm{I} = \frac{f}{Z_0}\mathrm{i}, \mathrm{J} = \frac{f}{Z_0}\mathrm{j}$

If values for $\epsilon_i$ are given, I and J can be acquired by solving a linear system for equations (9) and (10) because the other parameters were known values. Then, i and j are computed by normalizing I and J, respectively. This algorithm is POS. By repeating the POS algorithm with the newly acquired $\varepsilon_i$, more accurate values for I and J can be computed. This iterative procedure is

the POSIT algorithm. With an initial value of 0 for $\varepsilon_i$, optimal values for i, j and k (rotation matrix) can be computed within a few iterations using the POSIT algorithm.

2) Data acquisition

To record the NHP of the patient, ceramic sphere markers, which did not produce severe artifacts in the CT, were attached to the patient's face with transparent medical plastic tape. The sphere markers were evenly distributed on the maxillofacial area where facial soft tissue showed no severe transformation while acquiring the CT image to increase the accuracy of the POSIT algorithm. The patient's head was relaxed and positioned to NHP and the height and level of a tripod, where a camera was mounted, were adjusted to horizontally face the patient's maxillofacial area. Photographs of the patient were taken with a digital camera (Nikon D300, Nikon corporation., Tokyo, Japan) while the patient stood upright with NHP and facing directly the camera. The CT of the patient was taken with the markers attached on the face immediately after the photography was taken.

3) Application of the POSIT algorithm

The positions of the sphere markers were identified in the photograph and CT image, respectively. The two-dimensional center positions

of the markers ($x_i$, $y_i$) were acquired from the photograph in pixel units, and the 3-dimensional marker positions ($X_i$, $Y_i$) were acquired in the CT coordinate. The origin of the 2-dimensional photograph image was determined as the center of the image. These two position data were applied to the POSIT algorithm to calculate the NHP from the 2-dimensional photograph. Focal length ($f$) of the camera in pixel unit was calculated by the following equation. In this study, the image width was 3216 pixels and the focal length was 105mm and CCD width was 23.6 mm.

$$f = \frac{\text{Image width in pixels} \times \text{foal length in mm}}{\text{CCD width of camera in mm}} \quad (11)$$

According to the equation 11, $f$ was 14308.47 pixels and all the required data including marker position and $f$ value were used to calculate the POSIT algorithm. As a result of the POSIT algorithm, the amount of rotation required for the CT data to simulate NHP was acquired in the rotation matrix form and applied to the CT data.

4) Phantom for accuracy evaluation

A phantom was produced to evaluate the accuracy of the NHP recording and simulation method. The phantom was composed of 3 parts; a

skull model, acrylics stand, and rotation stage with 3 degree of freedom (Figure 3). A skull model was mounted on the acrylic stand which was designed to guarantee firm fixation to the rotation stage by fastening bolts. Four sphere markers (diameter: 1mm, stainless steel) were attached to all the corners of the top side of the tetragonal acrylic stand base for the accuracy evaluation. Lines connecting these metal spheres consisted of the x, y and z axes of the phantom coordinate system (Figure 4).

The overall procedure for NHP acquisition for the phantom was the same as the previously described NHP acquisition procedure for the patient case, but a few extra procedures were added for the phantom experiment. First, the phantom was positioned arbitrary in the CT coordinate while acquiring the CT data of the phantom so that the CT coordinate system mismatched with the phantom coordinate system. Second, before taking the photograph of the phantom, the rotation stage was adjusted to be parallel to the global horizontal using a spirit level (Figure 5). Then, an acrylic stand and a skull model were mounted on the rotation stage (Figure 6). This position was determined as the virtual NHP of the phantom. Ideally, in this virtual NHP, the phantom coordinate system was parallel to the global coordinate system. Next, by adjusting the camera tripod, the center of the photograph was set to be in the middle of the 2-dimensional distribution of the ceramic markers while the camera was kept parallel to the global horizon and orthogonal to the phantom.

This procedure guaranteed the ideally simulated virtual NHP of the CT data (phantom coordinate system) to be aligned with the CT coordinate system (global coordinate system).

5) Simulation of the natural head position

The acquired virtual NHP was applied to the CT data of the phantom and the phantom was reoriented in the virtual space (CT coordinate system). Orientation of the phantom in the virtual space was calculated based on the positions of the metal sphere markers attached to the acrylic base which determined the x, y and z axex of the phantom coordinate system in the virtual space (CT coordinate system). The degree of discrepancy (roll, pitch and yaw) between the reoriented phantom coordinate system and the virtual coordinate system (CT Coordinate system) was determined as an error of the developed NHP simulation method.

6) Accuracy evaluation

Ten photographs were taken at the first session and another 10 photographs were taken by the same observer **2** weeks later to evaluate the intra-observer variation. Another 10 photographs were taken by another observer to evaluate the inter-observer variation. One-sample t-test was performed to evaluate the accuracy of the method and paired t-test and

independent samples t-test were applied to evaluate intra and inter-observer variation, respectively, with a significance of 0.05 (*P*-value).

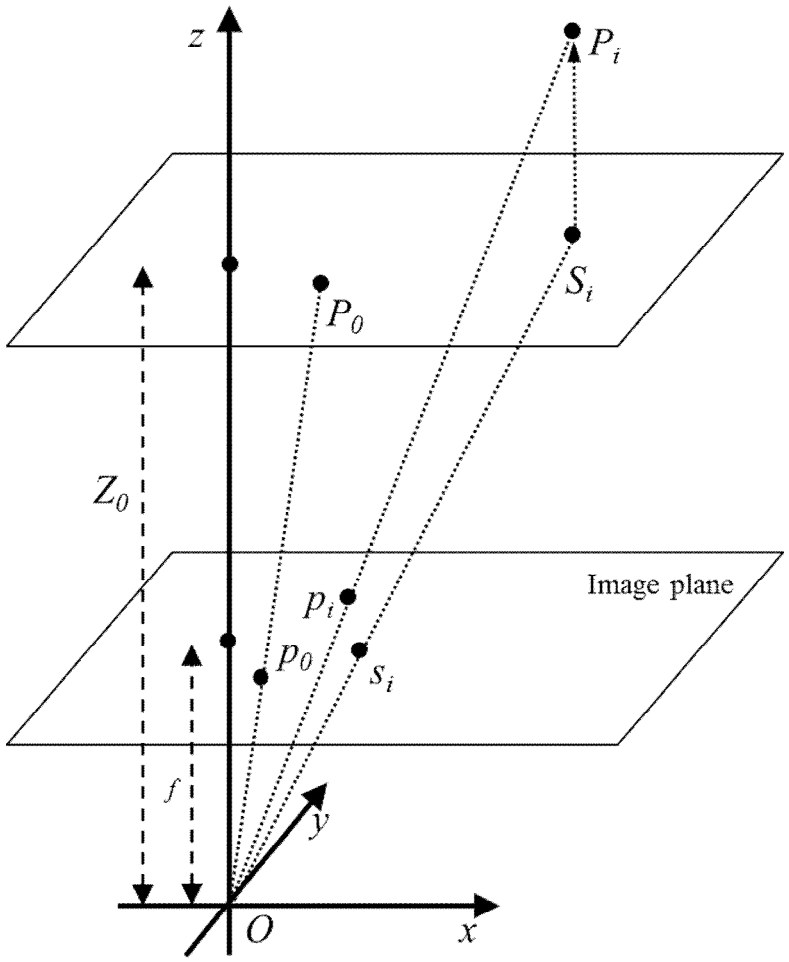


**Figure 2** Illustration of POSIT (Pose from Orthography and Scaling with Iteration) algorithm. Reference point for object: $P_0$, Feature points of the object with camera coordinates ($X_i$, $Y_i$, $Z_i$): $P_0, P_1, \ldots, P_i, \ldots, P_n$, Center of projection: O, Focal length: f. Scaled orthographic projection of $P_i$: $S_i$, Perspective projection of point $P_i$ and $S_i$ on the image plane: $p_i$ and $s_i$.

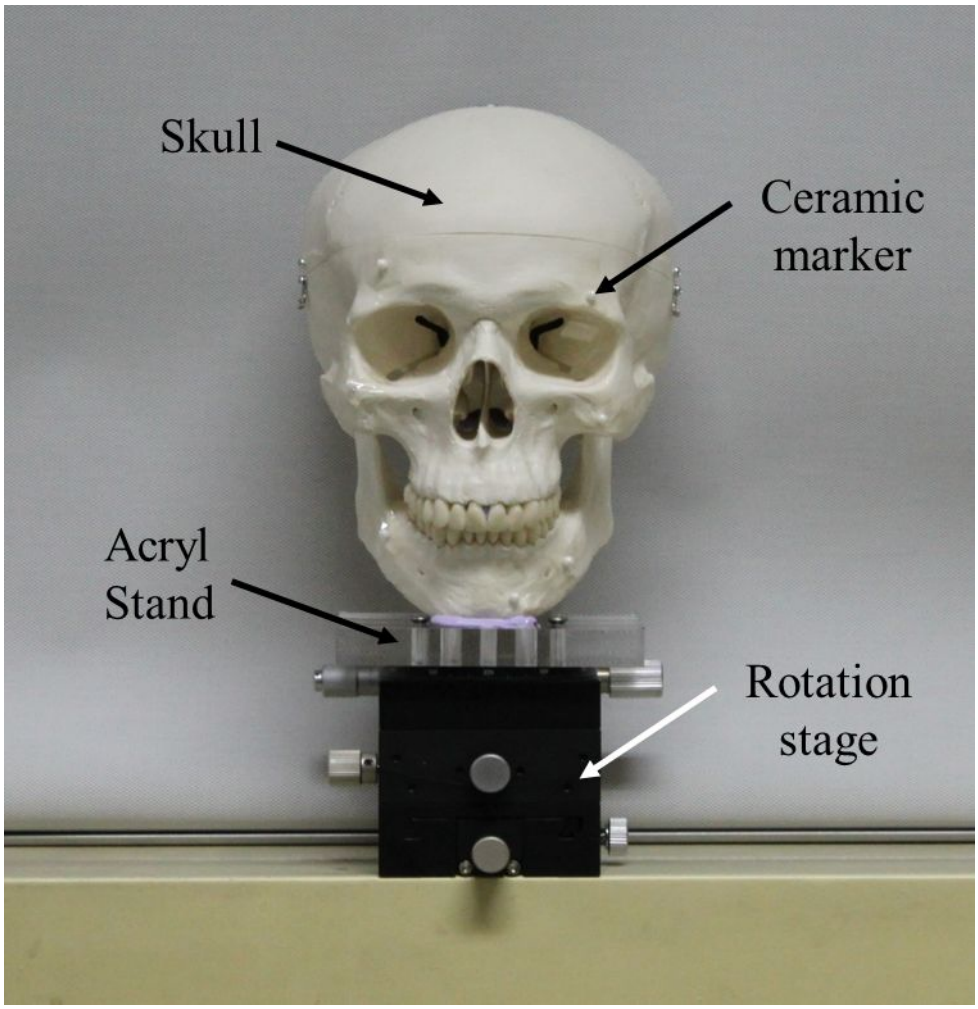


**Figure 3** Phantom for accuracy evaluation of natural head position simulation method.

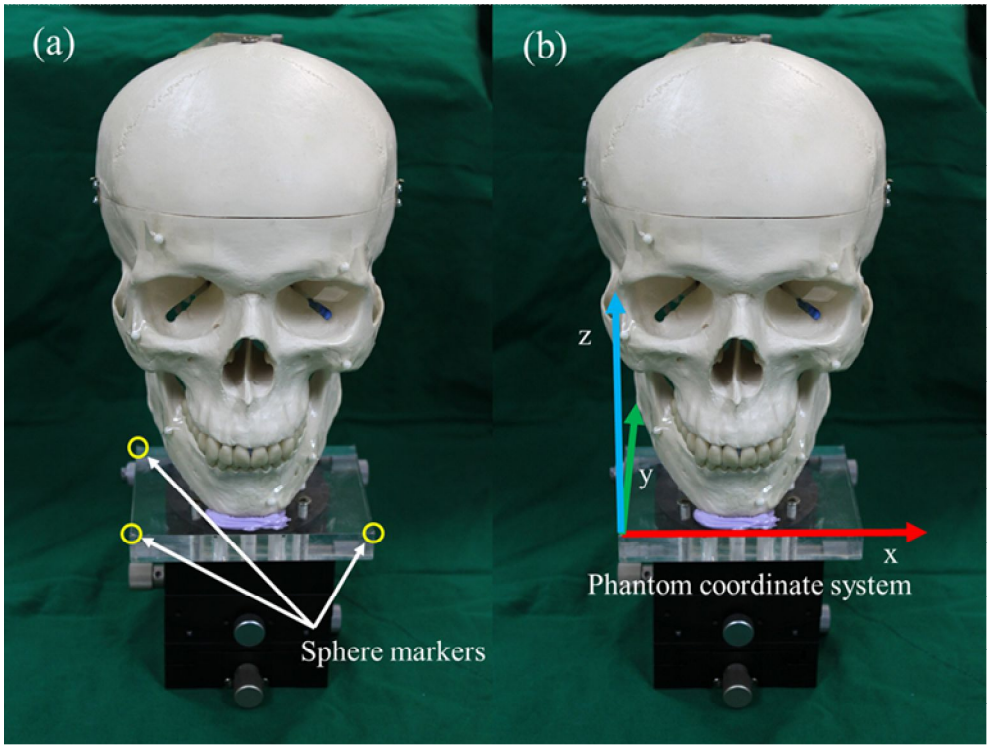


**Figure 4** (a) Sphere markers attached to the corners of the acrylic stand base.

(b) Phantom coordinate system constructed from the position of the markers.


**Figure 5** Rotation stage adjusted to be parallel to the global horizontal using a spirit level.

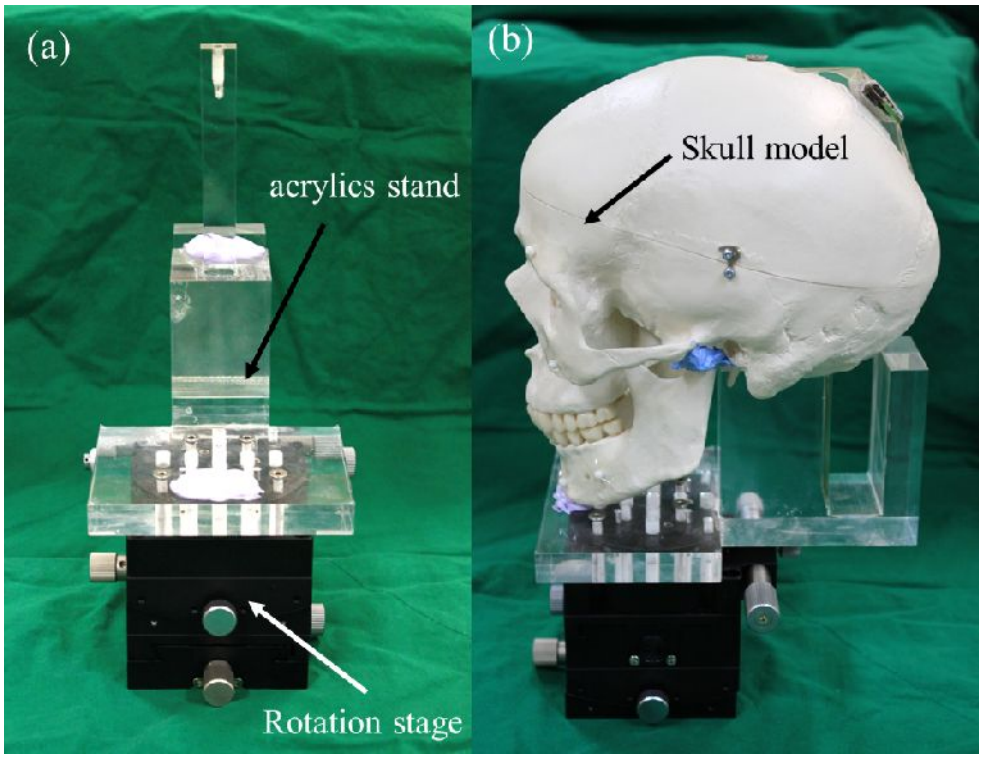


**Figure 6** (a) Acrylic stand for natural head position simulation accuracy evaluation. (b) Assembly of skull model and acrylic stand mounted on the rotation stage.

## 3. Surgery guide system

1) Model surgery and surgical splint

In conventional surgery, a dental splint was used to transfer the paper surgery result into the operation theatre. A dental splint was fabricated from the model surgery performed prior to the surgery. Dental casts were mounted on the articulator and the centric occlusion was reproduced relative to the Frankfort horizontal plane. Then, the maxilla cast was repositioned into the goal position according to the paper surgery. While the mandible cast remained in the same initial position, an intermediate splint was fabricated to reproduce the relative position between the maxilla and mandible. The intermediate splint was used to relocate only the maxilla bone segment to the goal position during the surgery. In two-jaw surgery, an additional splint called a final splint was produced to relocate the mandible bone segment after relocation of the maxilla to a desired position was completed. The final splint was fabricated through the model surgery after the maxilla and mandible cast were relocated to the planned final position. Although the final splint served as good guidance for the relocation of the mandible bone segment, the accuracy of the mandible relocation was crucially dependent on the exact relocation of the mandible bone segment. Positioning of the maxilla bone

segment with an intermediate splint, however, had an inherent limitation becausse the mandible rotated and did not remain in the initial centric occlusion position during the surgery. A guide system for the positioning of the maxilla bone segment was required to ensure the exact relocation of not only the maxilla but also the mandible bone segment.

2) Tracking device

In this study, an orthognathic surgery guide system was developed to help the surgeon confirm the real-time position of the maxilla bone segment intra-operatively. The system used an optical tracking system (Polaris NDI, Northern Digital Inc. Ontario, Canada) to track the bone segment. Specially designed registration body and splint were used to correlate the physical coordinate system with the CT coordinate system (Figure 7). Registration sphere markers (1mm in diameter, stainless steel) were installed on the registration body and attached to the registration splint by LEGO blocks (LEGO Group, Billund, Denmark).

3) Registration body

The registration splint made of dental resin was obtained in centric occlusion in the same way as a conventional bite splint is produced, and an extra bar protruded from the splint to enable attachment of the registration

body. Additionally optical tracking marker for the optical tracking system was attached to the registration body to enable 3-dimensional tracking of the registration assembly. The registration body was specially designed to improve the convenience and efficiency of the registration procedure. The partial shape of the optical tracking marker was engraved on the adaptor of the registration body so that optical tracking marker could be attached to the registration body in the same position repeatedly (Figure 8). Therefore, the relative position between the registration body (registration sphere markers) and the optical tracking marker was fixed during repeated usage.

4) Registration procedure

Facial CT scanning was performed at 120 kVp and 80 mAs with slice thickness of 0.75 (Siemens SOMATOM Sensation 10, Munich, Germany) while the registration splint with the registration body was firmly mounted on the patient's teeth. After acquisition of the CT data, the point-to-point registration method was applied to find the relationship between the physical coordinate system and CT coordinate system. First, the 3-dimensional positions of the six sphere markers were identified in the CT data. Then, the corresponding physical position of the markers in the camera coordinate system were located using a probe tool (Figure 9). Here, the physical positions of the landmarks were calculated relative to the origin of

the NDI tracking marker and used for the registration procedure. The registration procedure was executed with these corresponding pairs of marker positions, and the transformation matrix between the two coordinate systems was acquired as a result. As previously mentioned, because the relative position between the optical tracking marker and the registration body (registration marker) was fixed and reproducible, once the physical position of the markers were acquired pre-operatively with a probe tool, the same physical position data of the markers could be repeatedly used for registration without having to measure the position intra-operatively again. After registration, 3-dimensional movement of the registration body assembly was tracked by the optical tracking camera system in the CT coordinate system.

The result of the bone segment relocation previously acquired from the virtual surgery planning system was loaded into the orthognathic surgery guide system. An additional tracking marker for head tracking (head tracking marker) was attached to the patient's head to cancel the movement of the patient's head and to observe pure maxilla bone segment movement. Registration was performed in a previously described manner and the head tracking marker and registration assembly were mounted onto the patient's body while the patient was in centric occlusion with the same occlusal relationship during the CT data scanning.

5) Acquisition of the initial maxilla position

After registration was completed, the registration body was detached from the registration assembly and the initial position of the head tracking marker and registration assembly (mandible tracking marker) was acquired to calculate the initial relative relationship between the maxilla tracking marker and the head tracking marker. In this study, the intermediate splint was slightly modified to include an extruding bar to attach the maxilla tracking marker in the same manner as the registration splint. Once the initial position was acquired, the registration splint was replaced with the intermediate splint and the assembly of the tracking marker and tracking marker adaptor was attached to the intermediate splint. Then, tracking of the maxilla started while the intermediate splint was firmly attached to the upper jaw. Real-time position of the maxilla could be acquired when the intermediate splint was firmly mounted on the maxilla teeth. Since the tracking marker could be attached to the same position on the intermediate splint through the tracking marker adapter, once the tracking procedure started, the tracking marker could be detached from the intermediate splint and attached only when the maxilla position needed to be acquired. Detachment of the tracking marker prevented the tracking marker from limiting the surgeon's field of view and operation during the surgery.

6) Maxilla relocation and tracking

After acquisition of the initial maxilla position relative to the head at the start of the maxilla tracking procedure, Le-Fort I osteotomy and maxilla bone segment relocation procedure followed. The surgery guide system helped the surgeon to verify the real-time position of the maxilla while the maxilla bone segment was relocated. In the conventional surgery procedure, the intermediate splint was mounted on the maxilla and mandible teeth and tied together with dental wire. The complex of the maxilla and mandible bone was relocated to the goal position while the surgeons checked the height measurement with a ruler and a caliper. After relocation was accomplished, the maxilla bone segment was fixed to the skull with plates and screws. Then, the tracking marker, which was detached during the osteotomy and relocation procedure, was reattached to the intermediate splint and the position of the maxilla bone segment was tracked. Surgeons could adjust the position of the maxilla checking the discrepancy between the planned position and current position shown on the surgery guide system because the plates were not firmly fixed and had flexibility for adjustment.

7) Transformation for maxilla tracking

The following is a detail description of the maxilla bone tracking procedure during relocation. First, the relationship between the physical and

CT coordinate system was calculated with the following equation:

$$ {}^{CT}_{Max\_R}T = {}^{CT}_{Tracker}T \times {}^{Tracker}_{Max\_R}T \quad (12) $$

, where *CT* was the CT coordinate system, *Tracker* was the tracking camera coordinate system and *Max_R* was the position of the maxilla tracking marker at the time of registration. Once the registration was completed, ${}^{CT}_{Max\_P}T$, the homogeneous transformation matrix of the maxilla tracking marker in the CT coordinate system, was calculated and served as a reference for the coordinate system transformation. As previously explained, the relative position of the head tracking marker to the maxilla tracking marker, ${}^{Max\_R}_{Head}T$ (*Head* was the head tracking marker), was acquired while the registration splint was still mounted on the patient's teeth. Once ${}^{Max\_R}_{Head}T$ was acquired, it served as a constant value to enable the replacement of the registration splint with the intermediate splint during the tracking maxilla procedure. Then, the registration splint was replaced with the intermediate splint and the maxilla tracking marker was attached to the intermediate splint. The intermediate splint was mounted to the upper jaw and before starting the maxilla tracking procedure, the initial position of the maxilla tracking marker relative to the head tracking marker, ${}^{Head}_{Max\_Pi}T$, was acquired again. Transformation of the maxilla tracking marker position was calculated with equation 13 as follows:

$$ {}^{Max\_R}_{Max\_Pi}T = {}^{Max\_R}_{Head}T \times {}^{Head}_{Max\_Pi}T \quad (13) $$

, where *Max_Pi* was the initial position of the maxilla tracking marker immediately after mounting the intermediate splint to the upper jaw. As a result, the relative movement of the maxilla tracking marker from the initial maxilla position at the time of registration was calculated. By applying the registration transformation (Equation 12), the position of the maxilla tracking marker in the CT coordinate system was acquired.

$$ {}^{CT}_{Max\_Pi}T = {}^{CT}_{Max\_R}T \times {}^{Max\_R}_{Head}T \times {}^{Head}_{Max\_Pi}T \quad (14) $$

Finally, the overall tracking procedure can be summarized as the following equation:

$$ {}^{CT}_{Max\_p}T = {}^{CT}_{Max\_pi}T \times {}^{Max\_pi}_{Max\_p}T \quad (15) $$

, where *Max_p* is the position of the maxilla tracking marker during the tracking procedure.

8) Real-time maxilla tracking

Three-dimensional surface model of the bone segment was loaded into the surgery guide system. Preoperatively, surgeons designated anatomical points of interest on the maxilla and these points were shown as spheres on the surface model. Surgery plan data acquired from the virtual surgery system was applied to the maxilla surface model and preoperative and goal position of the maxilla bone segment was visualized with different color in a virtual

environment. During the tracking procedure, the real-time maxilla position was acquired and the transformation matrix calculated from the aforementioned method was applied to the maxilla surface model. Because points of interest and the maxilla acted like a rigid body and hence moved together, the same transformation was applied to the points of interests on the maxilla to track the points of interest. Therefore, the goal position and real-time position of the multiple points on the maxilla could be tracked simultaneously and visualized by applying equation 15, the same one used for tracking the maxilla bone segment. The quantitative discrepancy between the goal position and current position of these points was calculated 3-dimensionally which helped the surgeon comprehend the current bone segment position and how much movement should be made to realize the goal position.

9) Accuracy evaluation: simple-condition experiment

The accuracy of the surgery guide system was evaluated and compared with the conventional surgery guide method by simulating a surgery procedure using dental cast and semi-adjustable articulator. Dental casts of the maxilla and mandible were fabricated and a registration splint for the dental casts was produced. Six sphere markers (1 mm in diameter, stainless steel) were installed in the maxilla dental cast as fiducial markers for

accuracy evaluation (Figure 10). A CT of the dental casts was taken while the registration assembly was firmly mounted on the casts. In this experiment, accuracy was evaluated only for maxilla movement because in the 2-jaw surgery, the mandible was relocated using a final splint but not with the surgery guide system. Virtual surgery was performed using the virtual surgery planning system and the planned position of the maxilla part was loaded onto the surgery guide system. The maxillary model was repositioned by translations in the x-, y-, and z-axes and by rotations in the roll, pitch, and yaw directions. The maxillary model was moved by +3mm and -3mm with respect to the mandibular model in each surgery planning (total of 12 surgeries). Before starting the surgery, we performed a registration to match the cast model's physical space with the CT image space. During surgery, the registration assembly was mounted on the maxilla cast and the head tracking marker was attached to the superior border of the articulator (Figure 11 (a). After registration was finished, the initial position of the 6 fiducial markers was recorded with a prove tool and tracking of the maxilla cast was started. The maxilla cast was relocated according to the virtual surgery plan by checking the visual and quantitative discrepancy information between the planed and real-time position of the maxilla cast and fiducial markers. After relocation was completed, the maxilla cast was fixed to the mandibular cast using bite impression material (Thixotropic vinyl polysiloxane, PARKELL

Inc., Edgewood, NY). The maxilla cast was kept in the desired goal position until the impression material was firmly hardened (Figure 11 (b)).

After relocation of the maxilla cast to the planed position, accuracy of the results was evaluated with two methods; the developed system error and conventional method error. First, the developed system error was determined as a 3-dimensional discrepancy between the planed and final position of the fiducial markers calculated by the system. Then, the conventional method error was acquired by the following procedure. The relocated positions of the fiducial markers installed in the maxilla cast were acquired using a prove tool and the displacement from the initial position was calculated (Figure 12). The difference between the acquired displacement and planned displacement was compared and determined as a conventional method error. Errors were calculated for each method from 5 measurements of relocated fiducial marker position for each axis (x, y, and z), and root mean square (RMS) error was also calculated. Student t-test ($p$-value = 0.05) was done to evaluate the difference between the two errors (developed system error and conventional method error). One-way analysis of variance (ANOVA) was also done to analyze the differentiability of the accuracy in the different surgeries.

10) Accuracy evaluation: clinical situation experiment

The performance of the surgery guide system was, also assessed in a more clinical situation by comparing the accuracy of the system with the result of the conventional model surgery. Dental casts of patients were used for the experiment and the registration body assembly was fabricated as previously described. The CT data of the dental casts was acquired with the registration body assembly. 3-dimensional surface models of the dental casts were reconstructed from the CT data and imported into the virtual surgery system. In the conventional model surgery, relocation of the cast according to the planning was implemented based on the coordinate system of the articulator, and this articulator coordinate system did not coincide with the CT coordinate system. Therefore, before the virtual surgery started, the CT data needed to be aligned with the articulator coordinate system to exactly transfer the surgery plan in the virtual surgery system. Registration between the CT and articulator coordinate system was done with the point-to-point registration method, the same technique used in the surgery guide system. The physical positions of the registration markers on the registration body were measured 3-dimensionally with a special measurement device equipped with 3 digital calipers and, on the device, the maxilla dental cast was mounted in the same orientation as the articulator. With the measurement device, 3-dimensional positions of the registration markers were measured in the articulator coordinate system (Figure 13). The positions of the markers in the CT

coordinate system were also acquired and registration between two coordinate systems was done. The result of the registration was applied to the virtual surgery system and the surface model of the dental cast was aligned with the articulator coordinate system, which guaranteed an exact transfer of the conventional surgery plan to the virtual surgery system (Figure 14).

Virtual surgery was performed according to the paper surgery plan and the result of the virtual surgery was transferred to the surgery guide system. The result of the model surgery was used to evaluate the accuracy of the system. First, the mandible dental cast was mounted on the articulator and the registration body assembly was placed between the maxilla and mandible cast to locate the maxilla dental cast at the initial preoperative position. Then, the surgery guide system started to track the position of the maxilla cast till the maxilla cast was transferred to the goal position according to the model surgery result. The goal position of the maxilla cast was realized by simply mounting the maxilla cast on the articulator because the maxilla cast used in the experiment was modified to show the result of the model surgery (Figure 15). The quantitative discrepancy between the virtual goal position and the actual position of the maxilla cast according to the model surgery was calculated for the 8 landmarks evenly distributed on the maxilla cast. A total of 7 model surgery cases were used for the accuracy evaluation and 5 measurements were performed for each land marks.

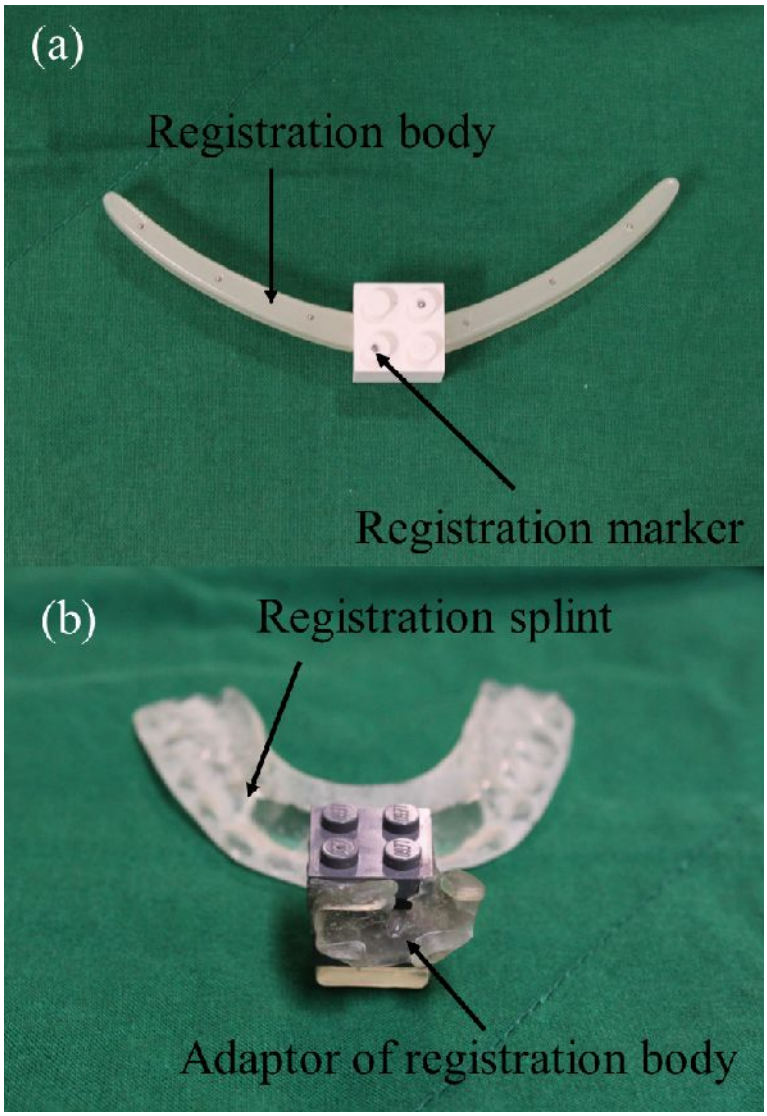


**Figure 7** (a) Developed registration body installed with registration markers.

(b) Registration splint with an adaptor for registration body fixation.

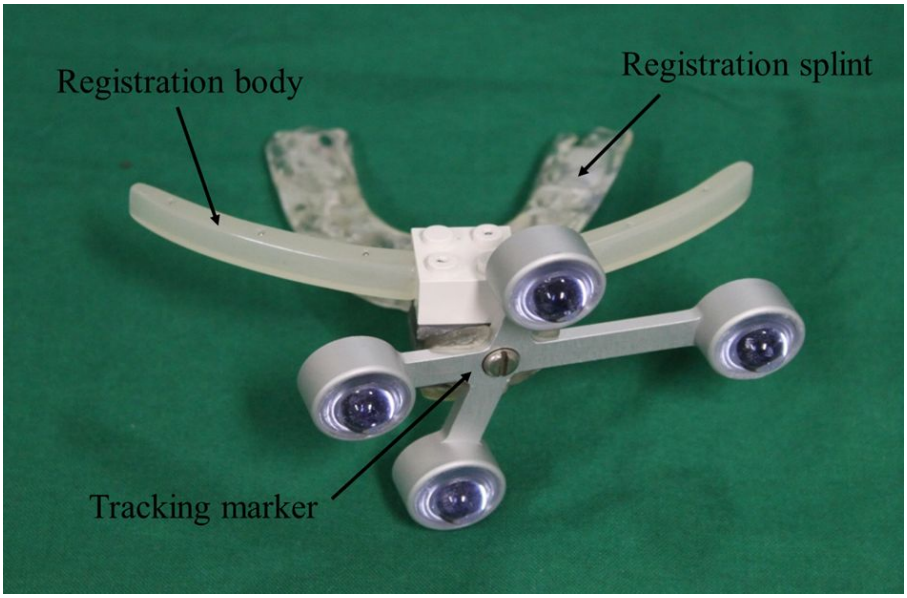


**Figure 8** Assembly of registration splint and registration body with registration markers.

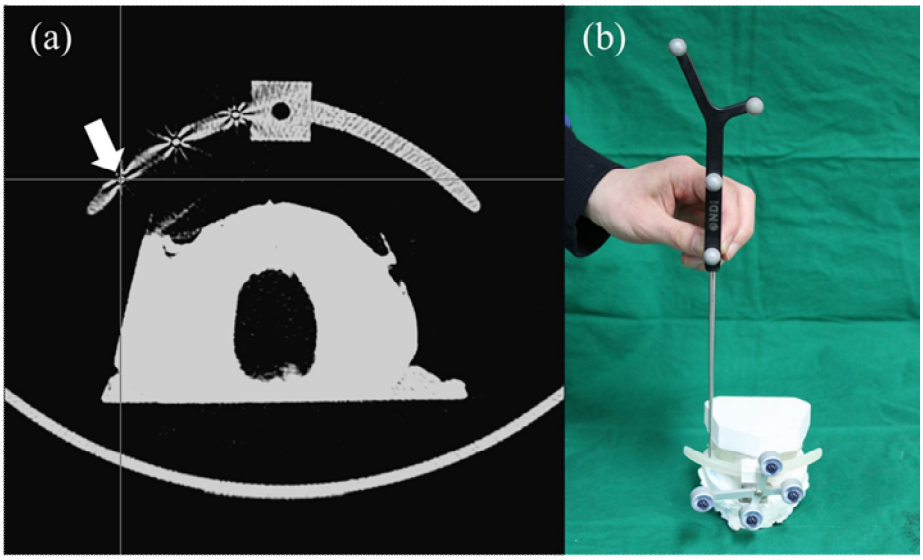


**Figure 9** Registration procedure by identifying registration marker position in CT coordinate system and physical (camera) coordinate system.

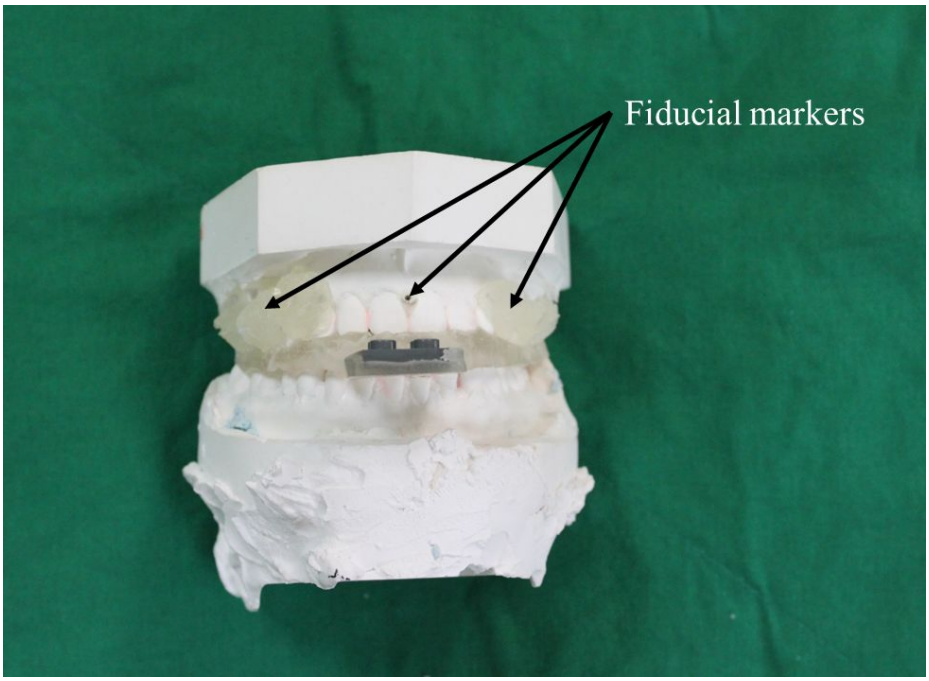


**Figure 10** Dental cast models with fiducial markers for surgery guide system accuracy evaluation

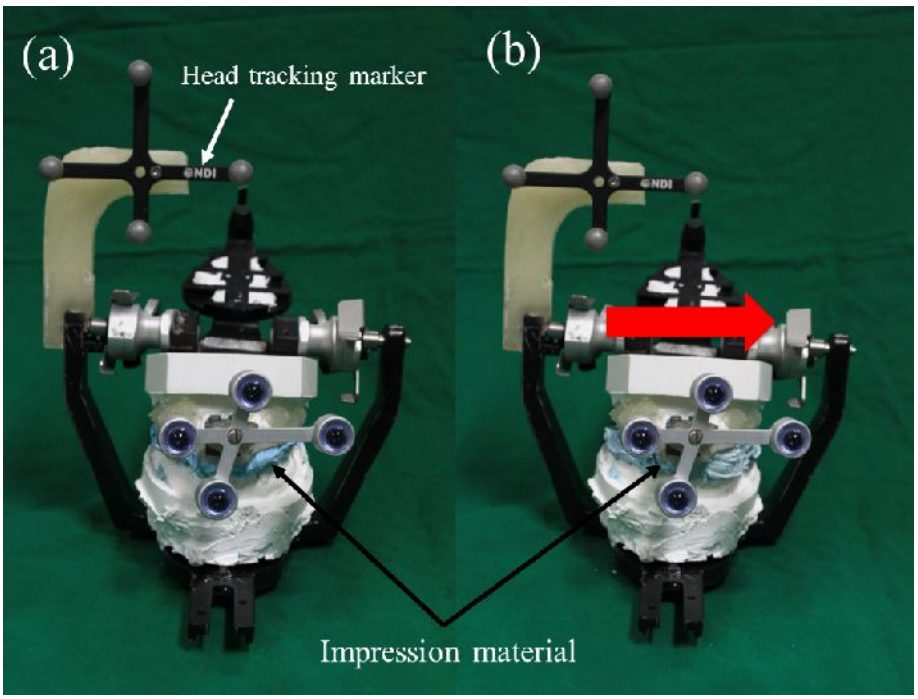


**Figure 11** Accuracy evaluation experiment of surgery guide system. (a) Initial position of the maxilla dental cast. (b) After relocation of the maxilla dental cast to the desired goal position.

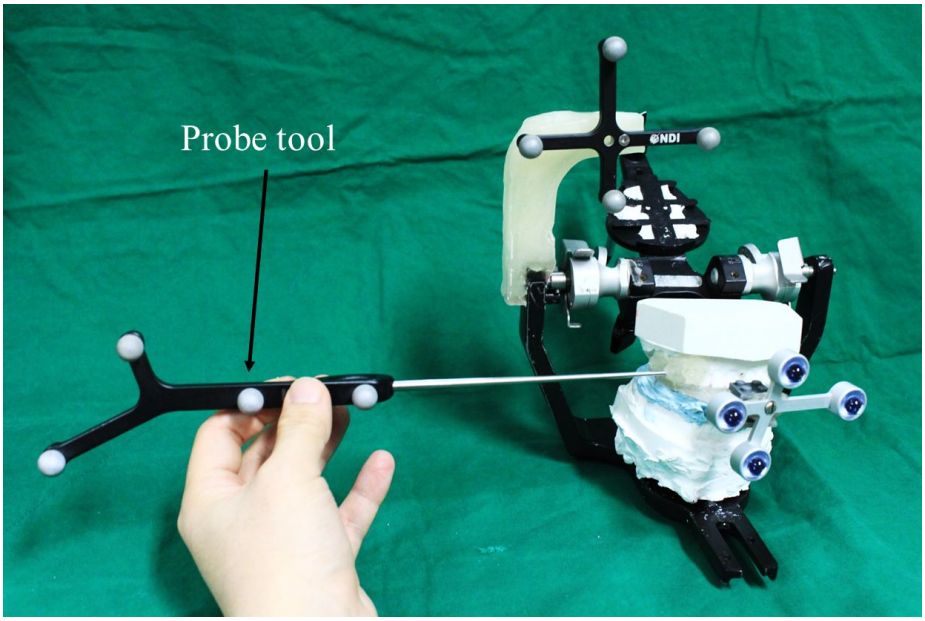


**Figure 12** Acquisition of the fiducial marker position using a probe tool after maxilla dental cast relocation procedure finished.

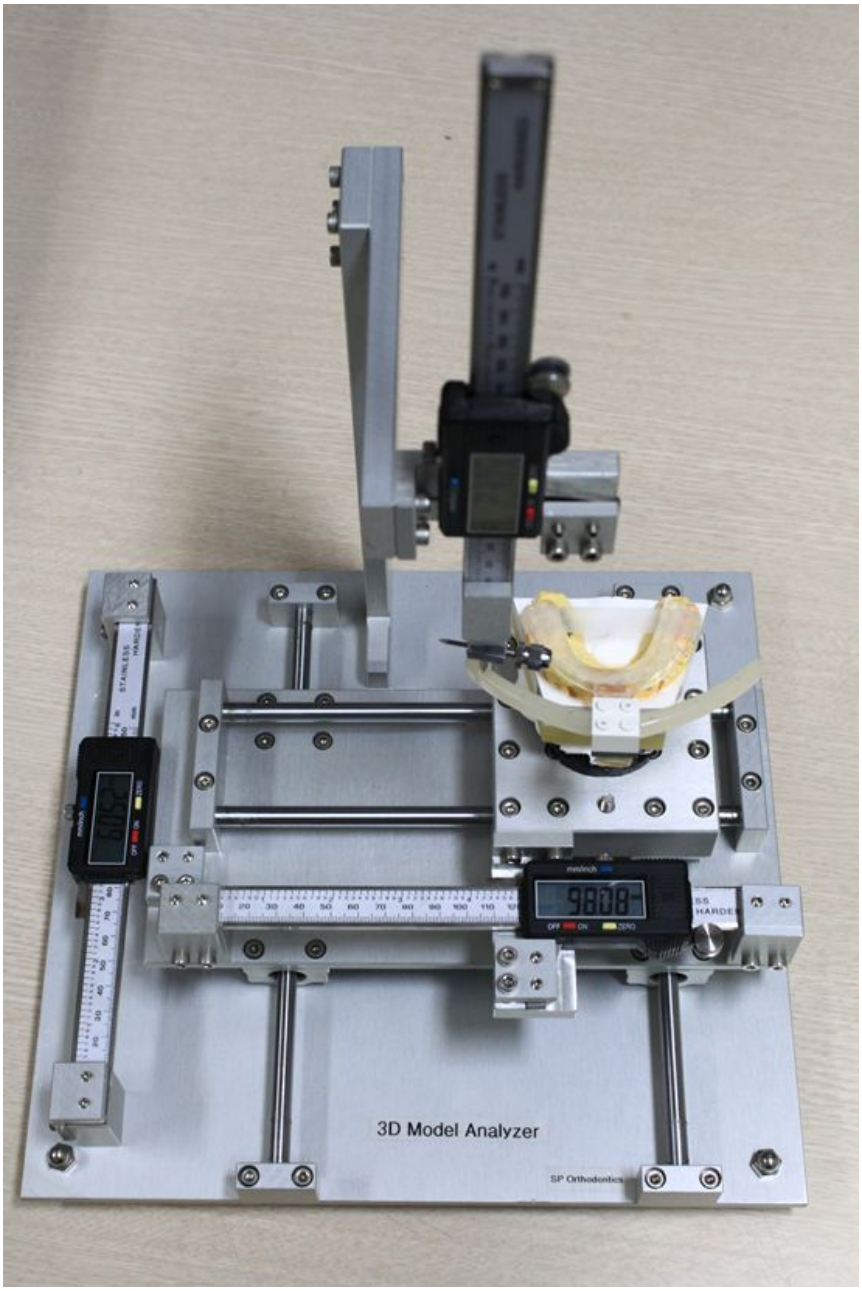


**Figure 13** Measurement of the physical position of the registration markers for the registration between the articulate coordinate system and CT coordinate system.

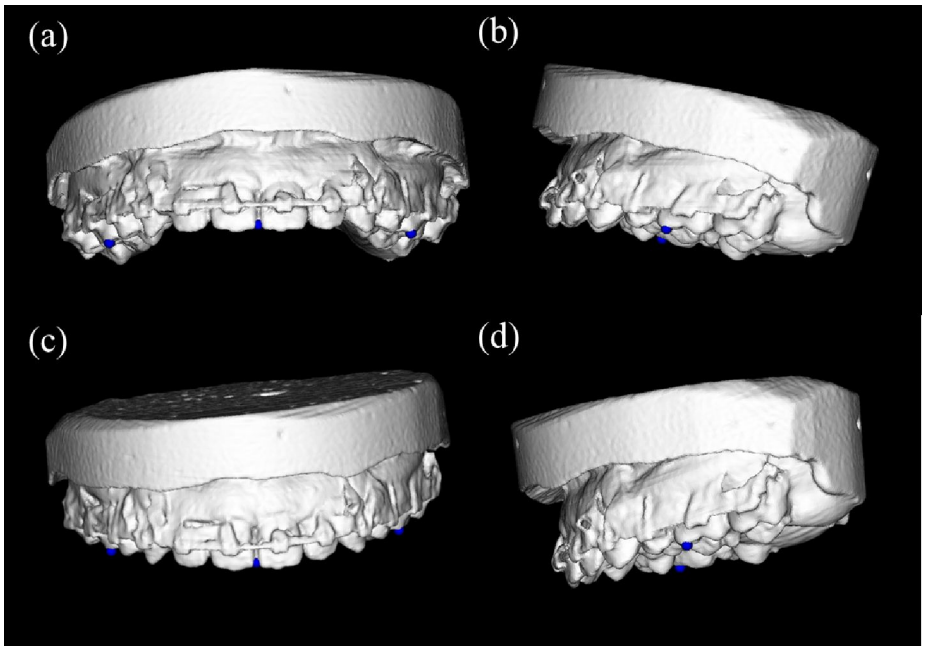


**Figure 14** Registration between the articulate coordinate system and CT coordinate system. Frontal (a) and lateral (b) view of the dental cast surface model in CT coordinate system. Frontal (c) and lateral (d) view of the dental cast surface model transformed to the articulate coordinate system.

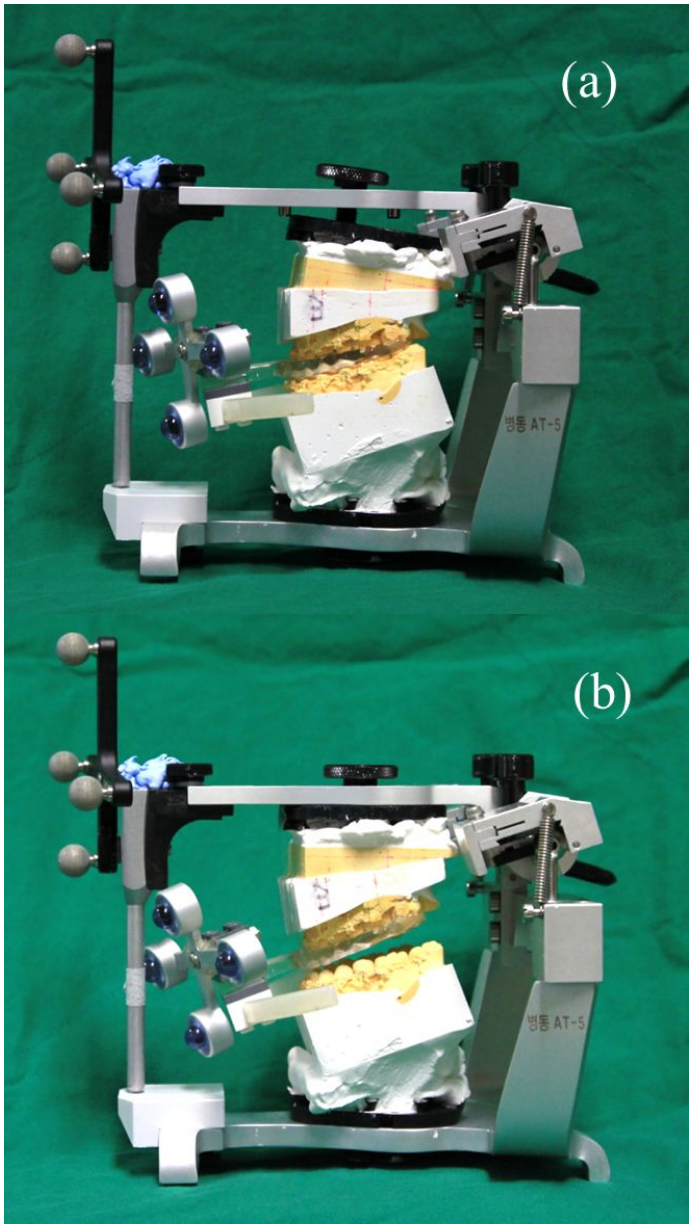


**Figure 15** (a) Pre-operative position of the maxilla dental cast (b) Relocated position of the maxilla dental cast according to the model surgery. Maxilla tracking tool was attached to the maxilla cast.

# RESULTS

## 1. Virtual surgery planning system

During the virtual surgery planning procedure, first, a virtual osteotomy was performed on a 3-dimensional skull model with a haptic device. A realistic osteotomy line was applied to the model with a combination of cutting curves and planes (Figure 16). Le-Fort I osteotomy was performed for the maxilla part. With the combination of the cutting planes and cutting curves, the maxilla and the lateral pterygoid plate was successfully resected (Figure 16 (a), (b) and (c)). SSOR osteotomy was implemented on the mandible and the ramus was segmented with the cutting curves (Figure 16 (d))

After the virtual osteotomy was completed, each bone segment model was loaded onto the virtual surgery planning system. Anatomical landmarks for planning were designated on the bone surface models as reference points for the bone relocation. According to the surgery plan, the maxilla model was relocated with a combination of rotational and translational movements by assigning quantitative movements of the predetermined reference landmarks

on the model. Accuracy of the maxilla relocation was verified by comparing the movements of the landmarks calculated by the system with the result of the conventional surgery plan for each step. After finishing the relocation of the bone segment, collision detection was performed between bone segments and the surgeon identified possible collision lines and areas pre-operatively. The result of the bone relocation and collision detection could be observed from various view points by freely rotating the model in 3-dimensional space (Figure 17).

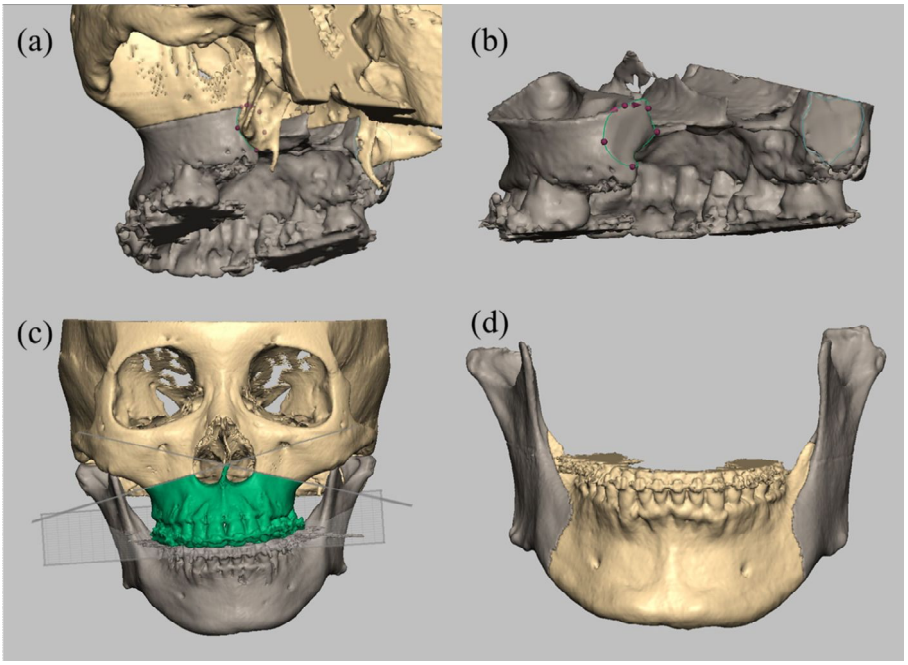


**Figure 16** Result of virtual osteotomy with a combination of cutting planes and curves. Cutting curves drawn along the lateral pterygoid plate (a) and the result of resection (b). Combination of cutting plane (c). Mandibular osteotomy with cutting curves (d).

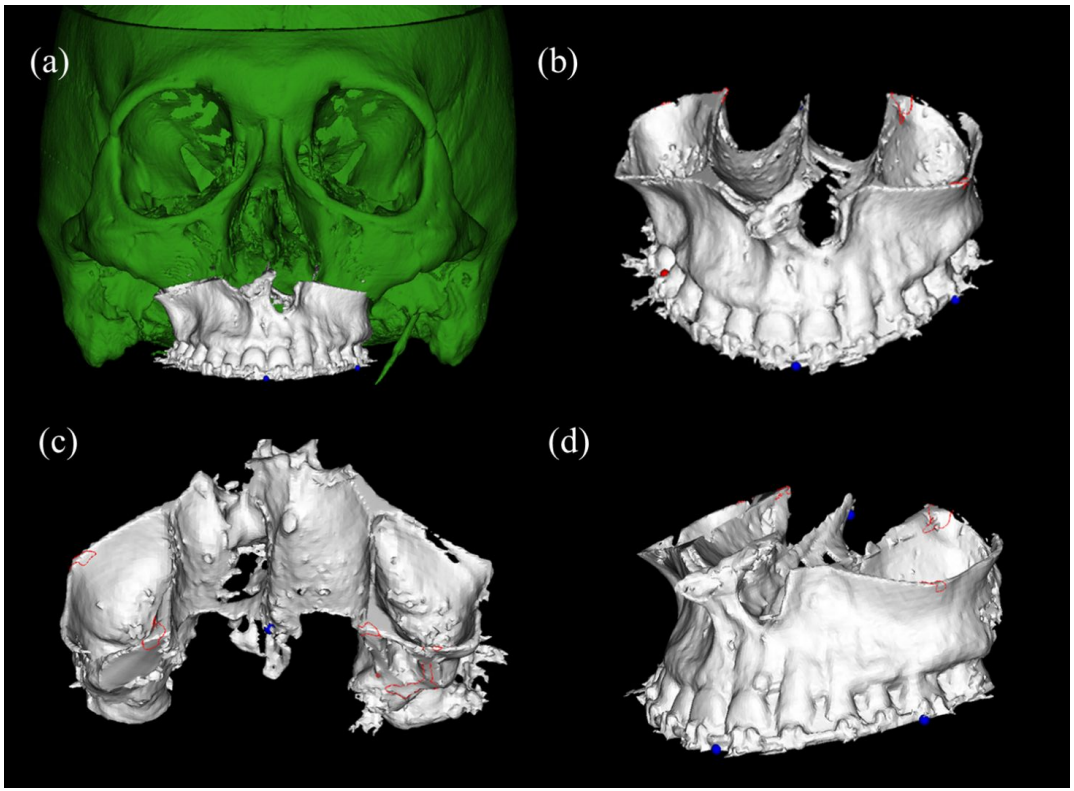


**Figure 17** Result of collision detection between the maxilla and skull model. The maxilla and mandible after relocation procedure finished (a). Observation of collision line (red) from various view point ((b), (c) and (d)).

## 2. Natural head position simulation

An accuracy evaluation of the NHP simulation with the POSIT algorithm was done with a phantom model. CT data of the phantom was acquired with ceramic sphere markers on the skull model, and the top surface of the rotational stage was aligned parallel to the global horizon, and this orientation was considered as the virtual NHP of the phantom. The camera was positioned to horizontally and orthogonally face the phantom while the center of the image was located in the middle of the maxillofacial area, where the ceramic markers were located. The 2-dimensional and 3-dimensional positions of the ceramic markers were acquired from the photograph and CT data, respectively. Using the POSIT algorithm, the virtual NHP of the phantom was acquired within a few iterations and applied to the surface model of the phantom reconstructed from the CT data (Figure 18). The positions of sphere markers attached to the base of the acrylic stand were acquired and the coordinate system of the phantom was calculated from the marker positions. The discrepancy between the CT and the phantom coordinate system, which was relocated to the virtual NHP, was determined as an error of the developed method.

Table 1 and 2 show the accuracy of the NHP simulation method.

According to the one-sample *t*-test (*p*-value=0.05), all measurements of NHP acquired by two observers were not significantly different from the virtual NHP in roll, pitch and yaw. The paired *t*-test (*p*-value=0.05) was applied to the two sets of measurements acquired separately with a 2-week interval by one observer and the result showed no statistical difference. In addition, there was no statistical difference between the measurements acquired by the two different observers according to the result of the independent *t*-test (*p*-value=0.05).

**Table 1** Accuracy evaluation of natural head position simulation using POSIT (Pose from Orthography and Scaling with Iteration) algorithm performed by first observer.

| Measurement | Error (degree) | | |
|---|---|---|---|
| | Roll | Pitch | Yaw |
| 1 | -0.22 | 0.32 | 0.13 |
| 2 | -0.06 | -0.34 | -0.17 |
| 3 | 0.05 | 0.18 | -0.45 |
| 4 | 0.03 | -0.35 | 0.29 |
| 5 | 0.30 | -0.16 | 0.05 |
| 6 | -0.26 | 0.24 | -0.33 |
| 7 | -0.25 | -0.24 | 0.50 |
| 8 | -0.05 | -0.85 | 0.21 |
| 9 | -0.20 | -0.06 | -0.20 |
| 10 | 0.16 | -0.56 | 0.02 |
| Total average (Mean±SD) | 0.05±0.19 | -0.18±0.37 | -0.01±0.29 |

**Table 2** Accuracy evaluation of natural head position simulation using POSIT (Pose from Orthography and Scaling with Iteration) algorithm performed by second observer.

| Measurement | Error (degree) | | |
|---|---|---|---|
| | Roll | Pitch | Yaw |
| 1 | -0.17 | -0.54 | 0.26 |
| 2 | -0.06 | 0.46 | -0.46 |
| 3 | -0.05 | -0.77 | 0.14 |
| 4 | 0.07 | 0.60 | 0.23 |
| 5 | -0.12 | 0.95 | -0.82 |
| 6 | -0.11 | -0.88 | -0.30 |
| 7 | -0.05 | -0.60 | -0.42 |
| 8 | -0.01 | -0.38 | 0.23 |
| 9 | -0.11 | -0.08 | 0.73 |
| 10 | 0.22 | -0.35 | 0.03 |
| Total average (Mean±SD) | -0.06±0.10 | -0.11±0.63 | 0.02±0.46 |

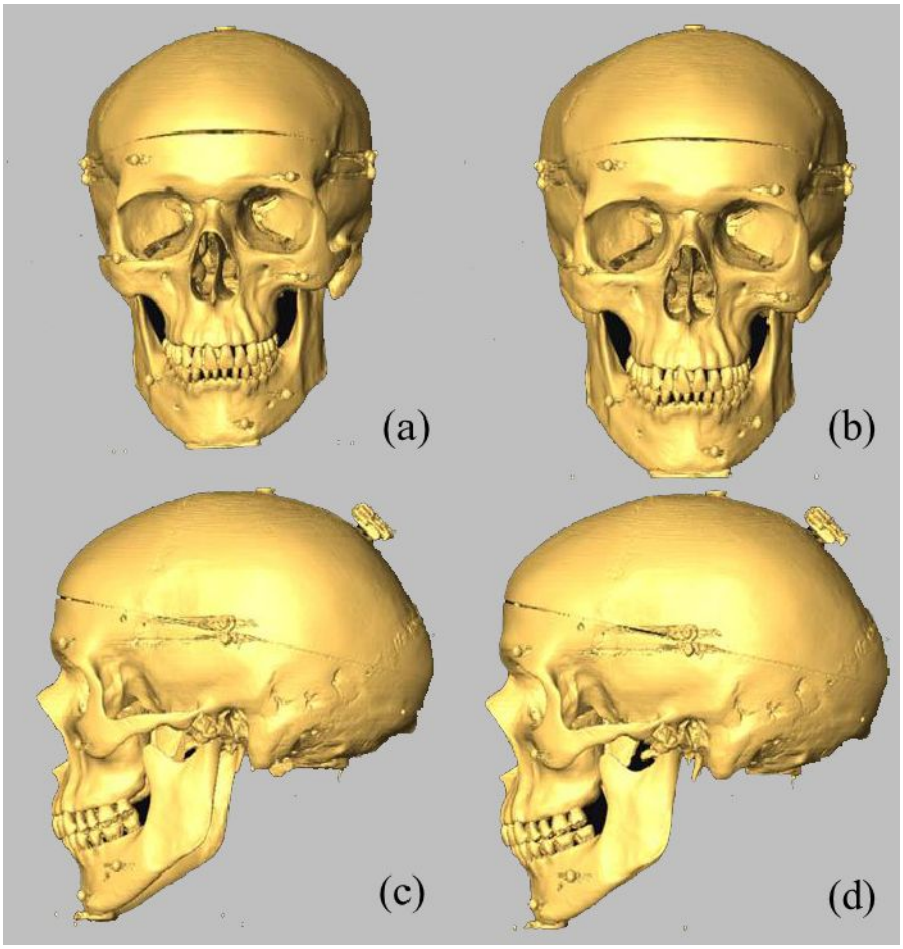


**Figure 18** Result of virtual natural head position simulation. Original data on the left side ((a) and (c)) and result of natural head position simulation on the right side ((b) and (d)).

## 3. Surgery guide system

An accuracy evaluation for the surgery guide system was done in a simple-condition experiment. The developed system error is presented in table 2 and the conventional method error acquired with a prove tool is shown in table 3. The mean accuracy was 0.47±0.22mm (range: 0.03 to 1.18mm) for the developed system error, and 1.06± 0.49mm (range: 0.11 to 3.14mm) for the conventional method error. According to the student *t*-test (*p*-value=0.05), there was a significant difference between two methods for all types of surgery. In all surgeries, the accuracy of the developed system was higher than that of the conventional method ($p<0.01$). Reproducibility as the standard deviation was also higher for the developed method than the conventional method in all surgeries (Table 3 and 4). An ANOVA test was also done to analyze the differentiability of the accuracies for the different surgeries. There were no significant differences in accuracy among the 12 surgery groups for the developed method ($p>0.05$). Regarding the accuracy of the conventional method, however, there were significant differences ($p<0.05$) that were classified into various subgroups according to a post-hoc test.

The accuracy of the system was also evaluated in a more clinical situation by using the result of the model surgery. After aligning the surface

model of the dental cast with the articulator coordinate system, the virtual surgery was performed according to the conventional surgery plan. The result of the virtual surgery was compared with the result of the model surgery by tracking the maxilla cast with the surgery guide system (Figure 19). The accuracy of the system was determined based on the discrepancy of the landmarks between the virtual surgery result and actual model surgery result. Average RMS error and absolute error (in mm) for each axis was calculated for 7 model surgery cases. A total of 5 measurements were done on the discrepancy of 8 landmarks for each case. Absolute error is presented in Table 5 ranging from 0.06 to 0.87 mm and the RMS error was 0.54±0.21 mm.

**Table 3** Accuracy evaluation result of the surgery guide system with developed method (Mean±SD) and maximum and minimum value of error.

| Movement | Mean±SD (mm) | Max.(mm) | Min.(mm) |
|---|---|---|---|
| X direction (+3mm) | 0.57±0.22 | 0.99 | 0.19 |
| X direction (-3mm) | 0.50±0.28 | 1.11 | 0.09 |
| Y direction (+3mm) | 0.48±0.23 | 0.95 | 0.13 |
| Y direction (-3mm) | 0.55±0.19 | 1.18 | 0.30 |
| Z direction (+3mm) | 0.45±0.26 | 0.92 | 0.05 |
| Z direction (-3mm) | 0.49±0.16 | 0.79 | 0.24 |
| Cant (+3mm) | 0.39±0.20 | 0.88 | 0.11 |
| Cant (-3mm) | 0.49±0.20 | 1.11 | 0.12 |
| Pitch (+3mm) | 0.39±0.29 | 1.04 | 0.07 |
| Pitch (-3mm) | 0.39±0.17 | 0.70 | 0.03 |
| Yaw (+3mm) | 0.46±0.19 | 0.88 | 0.12 |
| Yaw (-3mm) | 0.51±0.14 | 0.77 | 0.32 |
| Total average | 0.47±0.22 | 1.18 | 0.03 |

**Table 4** Accuracy evaluation result of conventional surgery guide method for maxillary orthognathic surgery (Mean±SD) and maximum and minimum value of error.

| Movement | Mean±SD (mm) | Max.(mm) | Min.(mm) |
|---|---|---|---|
| X direction (+3mm) | 1.41±0.68 | 3.14 | 0.42 |
| X direction (-3mm) | 1.29±0.50 | 2.44 | 0.43 |
| Y direction (+3mm) | 1.04±0.44 | 1.84 | 0.19 |
| Y direction (-3mm) | 1.14±0.63 | 2.77 | 0.14 |
| Z direction (+3mm) | 1.25±0.66 | 2.87 | 0.34 |
| Z direction (-3mm) | 1.04±0.38 | 1.95 | 0.35 |
| Cant (+3mm) | 0.81±0.33 | 1.69 | 0.28 |
| Cant (-3mm) | 1.10±0.48 | 2.38 | 0.46 |
| Pitch (+3mm) | 0.69±0.48 | 1.96 | 0.11 |
| Pitch (-3mm) | 1.04±0.38 | 1.75 | 0.29 |
| Yaw (+3mm) | 0.93±0.47 | 2.10 | 0.23 |
| Yaw (-3mm) | 0.94±0.36 | 1.70 | 0.23 |
| Total average | 1.06±0.4 | 3.14 | 0.11 |

**Table 5** Result of accuracy evaluation using model surgery. Average absolute error for each axis (Mean±SD) and RMS (root mean square) error (Mean±SD), and maximum (Max.) and minimum (Min.) value of error.

| Movement | Mean±SD (mm) | Max.(mm) | Min.(mm) |
|---|---|---|---|
| X direction | 0.23±0.11 | 0.57 | 0.06 |
| Y direction | 0.24±0.12 | 0.66 | 0.07 |
| Z direction | 0.34±0.19 | 0.87 | 0.08 |
| RMS error | 0.54±0.21 | 1.16 | 0.06 |

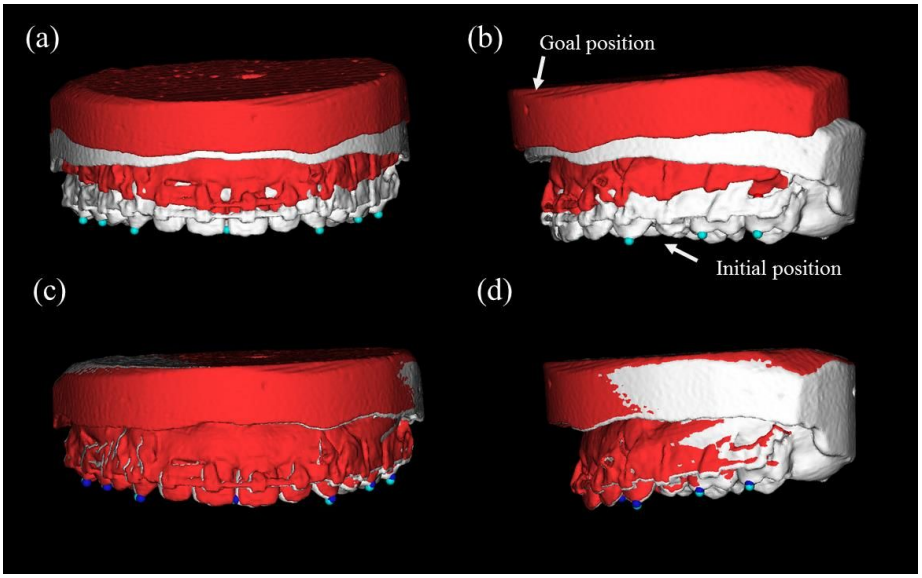


**Figure 19** Accuracy evaluation experiment using model surgery result. Planned goal position (red) and current position (white) of the maxilla bone segment. Frontal (a) and lateral (b) view of pre-operative initial position and frontal (c) and lateral (d) view of final position after relocation.


**Figure 20** Discrepancy between planned landmark position and current landmark position during bone tracking procedure. (a) Before relocation (b) After relocation according to the result of the model surgery.

# DISCUSSION

In this study, a virtual surgery simulation system including an NHP simulation and surgery guide system was developed and the accuracy of the system was evaluated. The result of the surgery planning was visualized 3-dimensionally and transferred to the surgery guide system. Virtual NHP was recorded using a digital camera and simulated on the 3-dimensional CT data. The surgery guide system enabled surgeons to perform surgery more accurately by confirming the intra-operative position of the bone segment visually and quantitatively.

## 1. Virtual surgery planning system

The developed virtual surgery system provided more accurate and useful information on the surgical outcome preoperatively. A conventional surgery plan was done based on a 2-dimensional cephalogram while the surgery was executed 3-dimensionally. Although model surgery was used to verify the result of the surgery pre-operatively, overall skeletal changes were hard to predict because only dental casts were used for the model surgery. The developed virtual surgery planning system implemented 3-dimensional virtual

surgery on a 3-dimensional bone surface model reconstructed from CT data. In previous studies on virtual surgery planning, virtual osteotomy was implemented in a simplified way by combining the cutting planes, which was not appropriate for the simulation of a real and complex osteotomy (14, 16). In this study, virtual osteotomy was performed on the 3-dimensional model and the osteotomy lines showed the real situation by combining the cutting curves and planes with the help of a haptic device which enabled more realistic and reliable virtual surgery planning. By drawing the cutting curves, the lateral pterygoid plate could be separated from the maxilla bone segment and an accurate simulation of Le-Fort I and SSRO osteotomy could be achieved.

The virtual surgery procedure followed the conventional planning method and provided the exact simulation for 2-dimensional planning in a 3-dimensional environment. A conventional surgery plan was simulated virtually by applying the step-by-step bone relocation procedure. Bone relocation was implemented based on the movements of the landmarks designated on the surface model. Virtual surgery was accurately performed by confirming the quantitative changes in landmark positions for each relocation step. Surgeons could observe the 3-dimensional result of the standard surgery planning and identify improvement in facial deformities pre-operatively. The quantitative positions of relocated bone segments were acquired because of

the virtual surgery and used for the surgery guide system. Collision detection between bone segments was executed and possible interference between bone segments according to the surgery plan could be identified pre-operatively. The improvement in virtual osteotomy enabled more accurate collision detection between bone segments. The result of the collision detection helped surgeons to predict possible region of collision that needed to be resected during the surgery operation.

## 2. Natural head position simulation

NHP has been considered as an ideal standard for evaluating facial morphology especially when patients have facial asymmetry. Most studies on NHP record have been implemented 2-dimensionally (34-38). Recent development in 3-dimensional medial imaging technology such as CT imaging has increased the need for simulating NHP on 3-dimensional data. During CT scanning, a patient is positioned in the supine position and the head of patient is randomly oriented. Therefore the patient's head in CT data does not reflect the ideal NHP. Previously, some studies have developed methods to simulate NHP 3-dimensionally (33, 48). NHP simulation using a laser scanner was reported to be accurate, but no quantitative information on

the accuracy is available (33, 48). A method using a digital orientation sensor also showed high accuracy with a mean difference in sub-degree (Roll: -0.01±0.18, Pitch: -0.01±0.109, Yaw:-0.014±0.191) compared to the result of the laser scanner method (33). However, these methods need an expensive laser scanner or an additional bulky orientation sensor. Although the method with an orientation sensor is relatively simple and has an accurate measurement ability, the CT was taken with specially designed bite tray mounted on the patient's teeth, which hindered the surgeon from observing the CT image of the undisturbed patient.

In this study, the result of the NHP simulation showed good accuracy (Roll: 0.05±0.19, Pitch: -0.18±0.37, Yaw: -0.01±0.29) with good repeatability according to the accuracy and intra-observer and Inter-observer variation evaluation. Only small ceramic sphere markers were attached to the patient's face and an ordinary digital camera was used to record the 3-dimensional NHP. The developed NHP simulation method has an acceptable accuracy and is inexpensive and simple to apply in routine clinical situations.

## 3. Surgery guide system

The surgery guide system helped surgeons to verify the accurate

transfer of the planned maxilla position to the surgical field. The optical tracking device enabled the quantitative tracking of the maxillary bone segment intra-operatively. In this study, the efficiency and convenience of the surgery was improved by the specially designed registration body assembly. In previously developed guide systems, registration procedure needed to be performed at the start of the surgery, which was time consuming procedure and one of the reasons surgeons were discouraged from adopting a surgery guide system in a clinical environment. We have designed the registration body assembly in a unique way such that the physical relationship between the registration marker and registration body is fixed. The registration marker could be repeatedly attached to a relatively fixed position to the registration body allowing for preoperative registration. Registration was completed by only applying the preoperatively saved data file of the registration marker position and there was no need to designate the marker position using a prove tool manually during the surgery.

In a previous study, the tracking marker was required to be attached to the registration splint to track the maxilla bone segment; hence, the intermediate splint needed to be replaced with the registration splint during the surgery in order to acquire the maxilla position (14), which decreased the efficiency of the surgical procedure. In this study, there was no need to replace the intermediate splint with the registration splint again to track the maxilla

bone segment because the reference for the maxilla tracking was changed from the maxilla tracking tool to the head tracking tool after the registration procedure was completed. Moreover, during the surgery, the maxilla tracking marker could be detached from the intermediate splint and attached only when the maxilla position needed to be confirmed**.** Detachment of the tracking marker from the intermediate splint improved the surgeons' efficiency because fixation of the maxilla tracking marker to the intermediate splint limited the surgeons' scope of activity and view during surgery. Thus, detachment of the tracking marker increased the efficiency of the surgery procedure including the osteotomy and bone segment relocation procedures.

After relocation of the maxilla, surgeons identified real-time discrepancy between the relocated maxilla position and planned position visually and quantitatively and adjusted the maxilla position according to the discrepancy information. Visual alignment between the current and planned position of the 3-dimensional model was not sufficient for surgeons to identify how much discrepancy exists between the current and planned positions. In this study, quantitative discrepancy information of the pre-defined multiple landmarks was provided which enhanced the surgeons' comprehension about the relocation procedure. The landmarks used for the discrepancy calculation was determined in advance based on the CT image during the surgery planning procedure. This enabled an operator to check the difference between

the actual and planned positions qualitatively and quantitatively without manual intervention during the surgery and thus, perform the surgery more accurately by recognizing the surgery progress conveniently and intuitively.

The accuracy of the tracking system was evaluated in two ways (simple-condition experiment and clinical situation experiment). First, in the simple-condition experiment, the accuracy of the system was compared with the conventional surgery guide system method. Generally, the target registration error (TRE), the distance between corresponding points in the CT and the physical coordinate system not used in the calculation of the registration, are measured to quantify the registration error from intraoperative image-guided methods. The positions of landmarks used for calculating the error were obtained by applying a prove tool to the physical positions. The TRE was reported to range from 1.13 mm to 3.79 mm according to the types of localizers and fixation method of the fiducial markers (49-55). Using the optical image-guidance system, the registration by implanted cranial fiducials had a higher accuracy (1.7±0.7mm) than any others by anatomic landmarks, adhesive fiducials, and surface matching during craniotomy (56). A recent study reported a TRE of 0.93±0.31mm for the anterior maxillary and zygomatic regions for registration using six anatomical landmarks (57). Chapuis et al. used a system that provided intraoperative assistance with a display showing jaw positions and 3-dimensional positioning guides during

surgery (14). A target deviation error of 1.1±0.91 mm was obtained by applying a tracked pointer (14). In this study, the mean accuracy (deviation error) of the manual localization method (conventional method error) was 1.06± 0.49 mm, which was similar to the previous experiments. Under the simple-condition experiment, the system had a higher accuracy than that of the conventional method with an acceptable accuracy for all kinds of surgery.

In the developed tracking method, the positions of multiple landmarks selected from the CT image before surgery were tracked without the operator's intervention during surgery. Any anatomical landmark could be designated as a target landmark because the tracking and localization of the landmark was performed based on only the 3-dimensional CT image. It is not easy to apply a probe tool manually to a deep anatomical landmark in conventional localization method. The offset error between true and pointed physical positions of landmarks occurs when manually applying the pointing tool to landmarks, and this error is further amplified when transforming the physical position into the image position. As a result, the mean accuracy of the developed method was higher than that of conventional method using a probe tool. The positioning of the landmarks by operator intervention was subject to larger errors. Moreover, reproducibility was also higher with the developed method than when using the conventional method. Operator intervention decreased the accuracy and reproducibility of localization when

applying a probe tool to physical landmarks.

In the simple-condition experiment, the accuracy of 12 types of surgeries with different repositioning directions showed no significant differences. Particularly, the rotational movements (roll, pitch and yaw) had similar accuracy to those of the simple translational movements. Generally, deformities in the roll, pitch and yaw rotations are more difficult to correct than simple translations. The repositioning of a bone segment in different directions could be performed with consistency in all the surgeries with the developed method. However, the accuracies when using the conventional probe tool localization method were significantly different among surgeries and, thus, were classified into various subgroups. The human errors associated with operator intervention from manually applying a probe tool randomly influenced the accuracy.

The system was also evaluated in a more clinical situation using the model surgery result of patients. Virtual surgery was exactly performed based on the conventional surgery plan. Movement of the landmarks for bone relocation was verified for each steps of the relocation movement. After relocation, the procedure was realized on the articulator using the result of the model surgery, and the surgery guide system tracked the final position of the maxilla dental cast. The RMS error of the tracking system was 0.54±0.21 mm for the clinical situation experiment and the error was similar with that of the

simple-condition experiment. In previous studies, a 2 mm error was reported to be a clinically acceptable margin for orthognathic surgery (58, 59). In this experiment, a virtual surgery plan was implemented in exactly the same way as real surgery planning consisting of a series of rotational and translational movements Except for the bone relocation procedure in the virtual surgery planning system, there were other factors causing errors shown on the evaluation result. First, the difference between the virtual surgery and model surgery could be caused by the landmark designation procedure. Landmarks were selected on the maxilla bone (teeth) to relocate the bone segment for both the virtual surgery and model surgery. Because the surgery consisted of a series of rotational and translational movements, errors in designating landmarks could accumulate through the relocation procedure and cause a discrepancy between the virtual surgery and model surgery result. Additionally, registration errors in the tracking system and the inaccuracy of the optical tracking system could lead to errors in the accuracy evaluation. Considering overall the errors that occurred during the tracking system evaluation experiment, the result of the experiment showed that the developed system had good accuracy for clinical use.

The intermediate splint has been used as good guidance for maxilla relocation. However, the intermediate splint has a critical limitation because the mandible, which is a reference for the intermediate splint, rotates in the

temporomandibular joint during the surgery (14). If the mandible rotates during the relocation procedure, the intermediate splint cannot guarantee exact transfer of the surgery plan. In this situation, the developed surgery guide system could be used to ensure the correct relocation of the maxilla, because in the guide system, tracking of the maxilla was irrelevant to the mandibular movement. As the result of the experiment showed that the tracking system could accurately track the goal position, the developed tracking system could be used as a verification tool for the accurate transfer of the surgery plan.

In conclusion, the developed system helped surgeons to predict and verify the result of orthognathic surgery pre-operatively. The method for recording and simulating the NHP was accurate and simple to adopt in routine clinical procedures. The surgery guide system gave surgeons visual and quantitative information on the intra-operative maxilla bone segment position. This system increased the efficiency and accuracy of orthognathic surgery from planning to the surgery procedure and could be useful in improving overall the facial deformities after surgery.

# REFERENCES


1. Aboul-Hosn CS, Hernández-Alfaro F. 3D planning in orthognathic surgery: CAD/CAM surgical splints and prediction of the soft and hard tissues results – Our experience in 16 cases. J Craniomaxillofac Surg. 2012;40(2):162-8.

2. Bell RB. Computer Planning and Intraoperative Navigation in Orthognathic Surgery. J Oral Maxillofac Surg. 2011;69(3):592-605.

3. Bell RB, Markiewicz MR. Computer-Assisted Planning, Stereolithographic Modeling, and Intraoperative Navigation for Complex Orbital Reconstruction: A Descriptive Study in a Preliminary Cohort. J Oral Maxillofac Surg. 2009;67(12):2559-70.

4. Bettega G, Cinquin P, Lebeau J, Raphaël B. Computer-assisted orthognathic surgery: Clinical evaluation of a mandibular condyle repositioning system. J Oral Maxillofac Surg. 2002;60(1):27-34.

5. Bettega G, Dessenne V, Raphaël B, Cinquin P. Computer-assisted mandibular condyle positioning in orthognathic surgery. J Oral Maxillofac Surg. 1996;54(5):553-8.

6. Gelesko S, Markiewicz MR, Weimer K, Bell RB. Computer-Aided

Orthognathic Surgery. Atlas Oral Maxillofac Surg Clin North Am. 2012;20(1):107-18.

7. Marmulla R, Mühling J. Computer-Assisted Condyle Positioning in Orthognathic Surgery. J Oral Maxillofac Surg. 2007;65(10):1963-8.

8. Mischkowski RA, Zinser MJ, Kübler AC, Krug B, Seifert U, Zöller JE. Application of an augmented reality tool for maxillary positioning in orthognathic surgery – A feasibility study. J Craniomaxillofac Surg. 2006;34(8):478-83.

9. Ellis E 3rd. Accuracy of model surgery: evaluation of an old technique and introduction of a new one. J Oral Maxillofac Surg 1990;48(11):1161-7.

10. Proffit WR, White RP, Sarver DM. Contemporary treatment of dentofacial deformity. St Louis: Mosby; 2002.

11. Turvey T, Hall DJ, Fish LC, Epker BN. Surgical-orthodontic treatment planning for simultaneous mobilization of the maxilla and mandible in the correction of dentofacial deformities. Oral Surg Oral Med Oral Pathol. 1982;54(5):491-8.

12. Sohmura T, Hojo H, Nakajima M, Wakabayashi K, Nagao M, Iida S, et al. Prototype of simulation of orthognathic surgery using a virtual reality haptic device. Int J Oral Maxillofac Surg. 2004;33(8):740-50.

13. Bettega G, Payan Y, Mollard B, Boyer A, Raphaël B, Lavallée S. A simulator for maxillofacial surgery integrating 3D cephalometry and

orthodontia. Comput Aided Surg 2000;5(3):156-65.

14. Chapuis J, Schramm A, Pappas I, Hallermann W, Schwenzer-Zimmerer K, Langlotz F, et al. A new system for computer-aided preoperative planning and intraoperative navigation during corrective jaw surgery. IEEE Trans Inf Technol Biomed 2007;11(3): 274-87.
15. Girod S, Teschner M, Schrell U, Kevekordes B, Girod B. Computer-aided 3-D simulation and prediction of craniofacial surgery: a new approach. J Craniomaxillofac Surg 2001;29(3):156-8.
16. McCormick SU, Drew SJ. Virtual Model Surgery for Efficient Planning and Surgical Performance. J Oral Maxillofac Surg. 2011;69(3):638-44.
17. Song KG, Baek SH. Comparison of the accuracy of the three-dimensional virtual method and the conventional manual method for model surgery and intermediate wafer fabrication. Oral Surg Oral Med Oral Pathol Oral Radiol Endod. 2009;107(1):13-21.
18. Tepper OM, Sorice S, Hershman GN, Saadeh P, Levine JP, Hirsch D. Use of virtual 3-dimensional surgery in post-traumatic craniomaxillofacial reconstruction. J Oral Maxillofac Surg 2011;69(3):733-41.
19. Troulis MJ, Everett P, Seldin EB, Kikinis R, Kaban LB. Development of a three-dimensional treatment planning system based on computed tomographic data. Int J Oral Maxillofac Surg 2002;31(4):349-57.
20. Uechi J, Okayama M, Shibata T, Muguruma T, Hayashi K, Endo K, et al.

A novel method for the 3-dimensional simulation of orthognathic surgery by using a multimodal image-fusion technique. Am J Orthod Dentofacial Orthop 2006;130(6):786-98.

21. Westermark A, Zachow S, Eppley BL. Three-dimensional osteotomy planning in maxillofacial surgery including soft tissue prediction. J Craniofac Surg 2005;16(1):100-4.

22. Xia J, Ip HH, Samman N, Wang D, Kot CS, Yeung RW, et al. Computer-assisted three-dimensional surgical planning and simulation: 3D virtual osteotomy. Int J Oral Maxillofac Surg 2000;29(1):11-7.

23. Moorrees CFA. Natural head position—a revival. Am J Orthod Dentofacial Orthop. 1994;105(5):512-3.

24. Moorrees CFA, Kean MR. Natural head position, a basic consideration in the interpretation of cephalometric radiographs. Am J Phys Anthropol. 1958;16(2):213-34.

25. Foster TD, Howat AP, Naish PJ. Variation in cephalometric reference lines. Br J Orthod 1981;8(4):183-7.

26. Lundström A, Lundström F, Lebret LM, Moorrees CF. Natural head position and natural head orientation: basic considerations in cephalometric analysis and research. Eur J Orthod 1995;17(2):111-20.

27. Lundström F, Lundström A. Natural head position as a basis for cephalometric analysis. Am J Orthod Dentofacial Orthop

1992;101(3):244-7.

28. Cooke MS, Wei SH. The reproducibility of natural head posture: a methodological study. Am J Orthod Dentofacial Orthop 1988;93(4):280-8.

29. Lundström A, Lundström F, Lebret LM, Moorrees CF. Natural head position and natural head orientation: basic considerations in cephalometric analysis and research. Eur J Orthod 1995;17(2):111-20.

30. Weber DW, Fallis DW, Packer MD. Three-dimensional reproducibility of natural head position. Am J Orthod Dentofacial Orthop. 2013;143(5):738-44.

31. Cooke MS, Wei SH. Cephalometric errors: a comparison between repeat measurements and retaken radiographs. Aust Dent J. 1991;36(1):38-43.

32. Verma SK, Maheshwari S, Gautam SN, Prabhat KC, Kumar S. Natural head position: key position for radiographic and photographic analysis and research of craniofacial complex. J Oral Bio Craniofac Res. 2012;2(1):46-9.

33. Xia JJ, McGrory JK, Gateno J, Teichgraeber JF, Dawson BC, Kennedy KA, et al. A New Method to Orient 3-Dimensional Computed Tomography Models to the Natural Head Position: A Clinical Feasibility Study. J Oral Maxillofac Surg. 2011;69(3):584-91.

34. Cleall JF, Alexander WJ, McIntyre HM. Head posture and its relationship to deglutition. Angle Orthod. 1996;36(4):335-50.

35. Huggare JA. A natural head position technique for radiographic cephalometry. Dentomaxillofac Radiol. 1993;22(2):74-6.

36. Showfety KJ, Vig PS, Matteson S. A simple method for taking natural-head-position cephalograms. Am J Orthod. 1983;83(6):495-500.

37. Uşümez S, Orhan M. Inclinometer method for recording and transferring natural head position in cephalometrics. Am J Orthod Dentofacial Orthop 2001;120(6):664-70.

38. Vig PS, Showfety KJ, Phillips C. Experimental manipulation of head posture. Am J Orthod 1980;77(3):258-68.

39. Arnett GW, Gunson MJ. Facial planning for orthodontists and oral surgeons. Am J Orthod Dentofacial Orthop 2004;126(3):290-95.

40. Cevidanes L, Oliveira AE, Motta A, Phillips C, Burke B, Tyndall D. Head orientation in CBCT-generated cephalograms. Angle Orthod 2009;79(5):971-7.

41. Polley JW, Figueroa AA. Orthognathic positioning system: intraoperative system to transfer virtual surgical plan to operating field during orthognathic surgery. J Oral Maxillofac Surg. 2013;71(5):911-20.

42. Kim DS, Choi SC, Lee SS, Heo MS, Huh KH, Hwang SJ, et al. Principal direction of inertia for 3D trajectories from patient-specific TMJ movement. Comput Biol Med. 2013;43(3):169-75.

43. Kim DS, Huh KH, Lee SS, Heo MS, Choi SC, Hwag SJ, et al. The

relationship between the changes in three-dimensional facial morphology and mandibular movement after orthognathic surgery. J Craniomaxillofac Surg. Epub 2013;DOI:10.1016/j.jcms.2013.01.
011.

44. Yang HJ, Kim DS, Yi WJ, Hwang SJ. Reduced joint distance during TMJ movement in the posterior condylar position. J Craniomaxillofac Surg. Epub 2013;DOI: doi:10.1016
/j.jcms.2012.12.005.

45. Kim DS, Choi SC, Lee SS, Heo MS, Huh KH, Hwang SJ, et al. Correlation between 3-dimensional facial morphology and mandibular movement during maximum mouth opening and closing. Oral Surg Oral Med Oral Pathol Oral Radiol Endod 2010;110(5): 648-56.

46. Kim SG, Kim DS, Choi SC, Lee SS, Heo MS, Huh KH, et al. The relationship between three-dimensional principal rotations and mandibular deviation. Oral Surg Oral Med Oral Pathol Oral Radiol Endod 2010;110(5):e52-60.

47. Dementhon DF, Davis LS. Model-based object pose in 25 lines of code." Int J Comput Vision 1995;15(1-2):123-41.

48. Xia JJ, Gateno J, Teichgraeber JF. New Clinical Protocol to Evaluate Craniomaxillofacial Deformity and Plan Surgical Correction. J Oral Maxillofac Surg. 2009;67(10):2093-106.

49. Benardete EA, Leonard MA, Weiner HL. Comparison of frameless stereotactic systems: accuracy, precision, and applications. Neurosurgery 2001;49(6):1409-15.

50. Eggers G, Senoo H, Kane G, Mühling J. The accuracy of image guided surgery based on cone beam computer tomography image data. Oral Surg Oral Med Oral Pathol Oral Radiol Endod. 2009;107(3):e41-8.

51. Metzger MC, Rafii A, Holhweg-Majert B, Pham AM, Strong B. Comparison of 4 registration strategies for computer-aided maxillofacial surgery. Otolaryngol Head Neck Surg. 2007;137(1):93-9.

52. Seeberger R, Kane G, Hoffmann J, Eggers G. Accuracy assessment for navigated maxillo-facial surgery using an electromagnetic tracking device. J Craniomaxillofac Surg. 2012;40(2):156-61.

53. Strong EB, Rafii A, Holhweg-Majert B, Fuller SC, Metzger MC. Comparison of 3 optical navigation systems for computer-aided maxillofacial surgery. Arch Otolaryngol Head Neck Surg. 2008;134(10):1080-4.

54. Zhang W, Zhang W, Wang C, Shen G, Wang X, Cai M, et al. A novel device for preoperative registration and automatic tracking in cranio-maxillofacial image guided surgery. Comput Aided Surg 2012;17(5):259-67.

55. Zhang W, Wang C, Yu H, Liu Y, Shen G. Effect of fiducial configuration

on target registration error in image-guided cranio-maxillofacial surgery. J Cranio Maxill Surg 2011;39(6):407-11.

56. Mascott CR, Sol JC, Bousquet P, Lagarrigue J, Lazorthes Y, Lauwers-Cances V. Quantification of true in vivo (application) accuracy in cranial image-guided surgery: influence of mode of patient registration. Neurosurgery 2006;59(1 Suppl 1):ONS146-56.

57. Sun Y, Luebbers, HT, Agbaje JO, Schepers S, Vrielinck L, Lambrichts I, et al. Validation of anatomical landmarks-based registration for image-guided surgery: An in-vitro study. J Craniomaxillofac Surg. Epub 2012;DOI: 10.1016/j.jcms.2012.11.017.

58. Proffit WR, Turvey TA, Phillips C. The hierarchy of stability and predictability in orthognathic surgery with rigid fixation: an update and extension. Head Face Med 2007;3:21

59. Proffit WR, Turvey TA, Phillips C. Orthognathic surgery: a hierarchy of stability. Int J Adult Orthodon Orthognath Surg 1996;11(3):191-204.

# 초 록

## 악교정 수술에서 시뮬레이션 및 영상 가이드를 제공하는 통합 시스템

김대승
협동과정 방사선응용생명과학 전공
서울대학교 의과대학원

악교정 수술에서 정확한 악교정 수술 계획과 수술 이행은 성공적인 미적, 기능적 향상을 위한 중요한 요소이다. 그러나 기존의 악교정 수술은 2차원 두부규격 방사선 사진을 기준으로 수술 계획이 이루어지며 술자의 경험과 기술에 의존한다는 제한점을 가지고 있다. 이러한 한계를 극복하기 위하여 악교정 가상 수술 계획에서부터 수술 가이드 시스템에 이르는 통합적 시스템이 개발되었다. 더불어 POSIT 알고리즘을 이용한 새로운 3차원 자연 두부 위치 재현 방법도 개발되었다. 또한 개발된 자연 두부 위치

재현 방법과 수술 가이드 시스템에 대한 정확도 평가를 실시하여 시스템의 임상적 활용성을 확인하였다.

가상 수술 계획 시스템에서는 햅틱 장비를 이용하여 CT 데이터로부터 생성된 3차원 표면 모델에 대해 현실적인 가상 골절술을 시행하였다. 생성된 골편 모델 위에 골편 재위치를 위한 표지자를 설정한 후 회전 및 병진 운동의 조합을 통해 가상 수술 계획을 재현하였다. 가상 수술은 전통적인 수술 계획 절차를 그대로 따라 진행되었으면 가상 수술 결과는 수술 가이드 시스템에 사용되기 위해 저장되었다.

자연 두부 위치 (natural head position) 재현을 위해 대상의 안면 부위에 세라믹 마커를 부착한 후 사진 촬영을 실시하였다. 마찬가지로 동일 위치에 마커를 부착한 상태에서 대상의 CT 데이터가 획득되었다. 2차원 사진 좌표계와 3차원 CT 좌표계간의 관계식을 구하기 위하여 POSIT 알고리즘이 적용되었다. 획득된 사진 데이터와 CT 데이터로부터 각각의 세라믹 마커들의 위치를 획득한 후 POSIT 알고리즘 계산에 사용하였고 그 결과로서 변환 관계식을 계산하였으며 계산된 변환 관계식은 CT 데이터에 적용되어 CT 데이터가 자연 두부 위치에 재위치 될 수 있었다.

자연 두부 위치 재현의 정확도를 평가하기 위한 모형을 제작하였다. 정확도 평가 결과 롤 (roll) 방향으로는 0.05±0.19°, 피치 (pitch) 방향으로는 −0.56±0.37°, 그리고 요 (yaw) 방향으로는 −0.01±0.29° 의 오차를 보였으며 이 수치는 임상적으로 허용 가능한 오차였다. 관찰자간 그리고 관찰자내 변이를 조사 결과 또한 유의한 차이를 보이지 않았다 ($p$−value = 0.05).

수술 가이드 시스템은 3차원 광학 추적 장비를 이용하여 상악 골편의 위치를 추적하였다. 수술의 효율성을 증대시키기 위한 정합용 도구가 특별히 제작 되었다. CT 좌표계와 실제 물리적 좌표계간의 정합이 실시되었고, 정합이 완료 된 후 상악 골편의 추적이 실시되었다. 가상 수술 계획 단계에서 생성된 수술 계획 데이터를 수술 가이드 시스템에 사용하였다. 상악 추적 절차 중 표지자들의 수술 계획 위치와 실제 수술 중 위치간의 차이를 3차원 표면 모델을 통해 가상 공간 상에 표현하였으며 또한 표지자들의 계획과 현재 위치간의 편차를 수치적으로 계산하여 제공하였다.

실험을 통해 수술 가이드 시스템의 정확도를 평가하고 기존 가이드 시스템 방법과 비교하였다. 개발된 시스템의 평균 오차는 0.47 ± 0.22 mm 이었고 기존 방법에 의한 오차는 1.05 ± 0.49

mm로 측정되었다. 모든 방향에 대해 개발된 시스템의 정확도가 통계적으로 유의하게 기존 방법보다 우수함을 확인할 수 있었다. 가이드 시스템의 정확도를 모델 수술 (model surgery) 결과를 활용하여 좀더 임상적인 조건에서 추가적으로 평가하였다. 정합용 도구를 장착한 상태에서 환자의 치아모형의 CT 데이터를 획득하였다. 모델 수술 시와 동일한 교합 상태를 재현하기 위해 CT 좌표계와 교합기 좌표계간의 정합을 실시하였으며 그 결과 가상 수술 시스템 상에서 상악 표면 모델의 위치를 교합 상태로 재위치 시킬 수 있었다. 실제 환자의 수술 계획에 따라 가상 수술이 시행되었으며 가이드 시스템을 통해 상악 치아 모형의 위치를 추적하였다. 가상 수술 결과에 따른 상악 표지자의 위치와 실제 모의 수술에 의한 상악 표지자의 위치 간의 편차를 수치적으로 계산하여 시스템의 정확도를 평가하였다. 총 7개의 모델 수술 결과에 대한 정확도 평가 결과 평균 절대 오차는 0.06에서부터 0.87 mm 였으며 평균 RMS (root mean square) 오차는 0.54 ± 0.21 mm로 임상적으로 허용 가능한 오차를 보였다.

본 연구에서는 악교정 수술 계획에서부터 자연 두부 위치 재현 및 악교정 수술 가이드 시스템에 이르는 통합적인 시스템을

개발하였다. 개발된 시스템을 통해 술자가 술전에 수술 결과를 예측하고 수술 중 수술 계획에 따른 정확한 이행 여부 판단할 수 있도록 도움을 받을 수 있었다. 결론적으로 개발된 시스템을 통해 수술 계획에서부터 이행에 이르는 전반적인 악교정 수술의 정확도와 효율성을 증대시킬 수 있었으며 또한 술 후 악안면 기형의 향상에 큰 도움이 될 수 있을 것으로 기대한다.

**주요어:** 악교정 수술, 자연 두부 위치 재현, 가상 수술 재현, 수술 가이드 시스템

**학번:** 2009-30596